

Building Efficient CNNs Using Depthwise Convolutional Eigen-Filters (DeCEF)

Yinan Yu Samuel Scheidegger Tomas McKelvey

Abstract

Deep Convolutional Neural Networks (CNNs) have been widely used in various domains due to their impressive capabilities. These models are typically composed of a large number of 2D convolutionals (Conv2Ds) layers with numerous trainable parameters. To reduce the complexity of a network, compression techniques can be applied. These methods typically rely on the analysis of trained deep learning models. However, in some applications, due to reasons such as particular data or system specifications and licensing restrictions, a pre-trained network may not be available. This would require the user to train a CNN from scratch. In this paper, we aim to find an alternative parameterization to Conv2D filters without relying on a pre-trained convolutional network. During the analysis, we observe that the effective rank of the vectorized Conv2D filters decreases with respect to the increasing depth in the network, which then leads to the implementation of the Depthwise Convolutional Eigen-Filter (DeCEF) layer. Essentially, a DeCEF layer is a low rank version of the Conv2D layer with significantly fewer trainable parameters and floating point operations (FLOPs). The way we define the effective rank is different from the previous work and it is easy to implement in any deep learning frameworks. To evaluate the effectiveness of DeCEF, experiments are conducted on the benchmark datasets CIFAR-10 and ImageNet using various network architectures. The results have shown a similar or higher accuracy and robustness using about $2/3$ of the original parameters and reducing the number of FLOPs to $2/3$ of the base network, which is then compared to the state-of-the-art techniques.

1 Introduction

Deep Convolutional Neural Network (CNN) is one of the most commonly used data-driven techniques. Typically, the large number of trainable parameters in deep learning models result in high demands on the computational power and memory capacities, which requires renting or purchasing expensive infrastructure for training. The heat generated by the GPU servers and the high power consumption during training is not environmentally friendly. Moreover, the size of the network and the number of floating point operations (FLOPs) play an important role for the inference process, where a small edge device may be used with restrictions on the complexity of the runtime. Therefore, building an efficient network is beneficial in terms of saving computational resources and reducing the overall cost for deep learning while achieving similar performances.

One topic on constructing an efficient CNN is the Neural Architecture Search (NAS), where the focus is to search for an optimal architecture given certain criteria. In this

paper, however, we assume that the wiring of the layers is pre-determined. Our focus is on how to improve the efficiency of a CNN for a given architecture.

There are mainly two strategies to achieve this. The first strategy is to take a pre-trained network and reduce the relatively insignificant parameters. This refers to as *compression* or *pruning* in the literature. This is often a desirable approach since many applications are using pre-trained networks as backbones in their networks.

However, in many scenarios, a pre-trained network is not available due to the particular data or system specifications, restrictive licensing, etc, where training a neural network from scratch is inevitable. In this case, after the overall architecture is established, one may re-parameterize the CNN to make it more efficient before training. That is, the network is still aimed to accomplish what the original CNN is supposed to achieve but with significantly fewer trainable parameters and FLOPs. The approximation is on the functional level instead of relying on trained parameters. This is the main focus of this work.¹

The main hypothesis for finding an efficient re-parameterization strategy is that there is significant redundancy in 2D convolutional (Conv2D) layers, which means that it may be sufficient to express a Conv2D layer with fewer parameters in order to achieve similar performances. One of the most commonly used function approximation techniques is the subspace low rank representation (Belhumeur et al. [4], Jolliffe [30], Golub and van Loan [12]). It is a family of very well studied and widely used techniques in the area of signal processing and machine learning. To put it in the context of CNN, the main idea is to rearrange the trainable variables into a vector space and find a subspace spanned by the most significant singular vectors of these variables. This new representation typically results in fewer trainable variables and runtime FLOPs with potentially better robustness.

There are two key steps involved to achieve this approximation: 1) find a **representative vector space** for each layer, and 2) estimate the **effective rank** without training. To find a representative vector space for Conv2D filters in a CNN, we have designed experiments where we observe that 1) vectorized Conv2D filters exhibit low rank behaviors, and 2) the effective ranks are different for each layer and they have a decreasing tendency with respect to the depth of the network. Given these observations, we propose a new convolutional filter Depthwise Convolutional Eigen-Filter (DeCEF). DeCEF is parameterized by a new hyperparameter we call rank, where a full rank DeCEF is equivalent to a Conv2D filter, whereas a rank one DeCEF is equivalent to a depthwise separable convolutional layer. To avoid the common problem of over-tuning, we use a rule-based approach for finding the ranks, where the rules are pre-determined by cross-validation on a small dataset trained on a small network. The rules are then applied to larger datasets and networks without further adjustments or tuning.

The paper is organized as follows. First, to motivate our work, we present the experiments and methodologies being used to observe and analyze the low rank behaviors in several trained CNNs in Sec. 2.1. We then propose the definition of a new type of filter parameterization DeCEF in Sec. 2.2. To further illustrate the advantages of using a DeCEF layer, we show two key properties, robustness and complexity, in Sec. 2.3. In Sec. 2.4, we present the training strategies for DeCEF. In Sec. 4, we show experiments to evaluate the effectiveness of DeCEF. First, we run ablation studies on the smaller dataset CIFAR-10 using DeCEF to gain empirical insights of its behaviors in Sec.4.2. To further evaluate the two properties of DeCEF, we conduct experiments

¹Although not being the main focus of this work, the proposed method can also be applied as a compression technique. This aspect is elaborated in the supplementary material.

using the benchmark network ResNet-50 1) on ImageNet for comparing complexity versus accuracy; and 2) on the corruption dataset ImageNet-C to validate the robustness of DeCEF. Moreover, in Sec. 4.3, we run further experiments on two additional popular network architectures DenseNet and HRNet. These results are also compared to other state-of-the-art model reduction techniques in Sec. 4.3.1.

2 DeCEF Layers

2.1 Motivation

First, let us formally define what a layer is in this context.

Definition 1. *In the scope of this paper, a Conv2D layer (or a **layer** for short)*

$$\mathcal{W} = \left\{ \mathbf{w}_j^{(i)} \in \mathbb{R}^{h \times h} : i = 1 \cdots c_{in}, j = 1 \cdots c_{out} \right\}$$

is a set of trainable units that are characterized by the following attributes: 1) number of input channels c_{in} ; 2) number of output channels c_{out} , and 3) parameterization: $\mathbf{w}_j^{(i)} \in \mathbb{R}^{h \times h}$, i.e. the Conv2D filter.

Note that there are multiple layers in a network, but we ignore the layer index in this definition for simplicity. When multiple layers appear in the same context, we use \mathcal{W}_l to denote the indexed layer, where the subscript $l \in \{1, \dots, L\}$ is the layer index and L is the **depth**² of the network. In addition, we denote $K := h^2$. Note that in practice, the filter shape may be rectangular. Moreover, for the sake of both consistency and convenience, we use i and j to denote the input channel index and the output channel index, respectively.

Our motivation of this work has originated from the low rank behaviors we have observed in the vectorized filter parameters, so let us start with this experimental procedure to illustrate our findings.

Procedure 1. *Observing low rank behaviors*

- Apply vectorization $\bar{\mathbf{w}}_j^{(i)} := \text{vec}(\mathbf{w}_j^{(i)}) \in \mathbb{R}^K$ and compute the truncated Singular Value Decomposition (SVD):

$$\bar{\mathbf{U}}^{(i)} \mathbf{S}^{(i)} \mathbf{V}^{(i)T} = \begin{bmatrix} \bar{\mathbf{w}}_1^{(i)} & \cdots & \bar{\mathbf{w}}_{c_{out}}^{(i)} \end{bmatrix}, \quad (1)$$

where matrices $\bar{\mathbf{U}}^{(i)}$ and $\mathbf{V}^{(i)}$ are the left and right singular matrix, respectively; and $\mathbf{S}^{(i)}$ is a diagonal matrix that contains the singular values in a descending order. The implementation of this procedure is well supported by any linear algebra libraries in most programming languages.

- Identify the effective rank for each input channel i :

$$r_i = |\{ \mathbf{S}^{(i)}[k, k] : \mathbf{S}^{(i)}[k, k] \geq \gamma \mathbf{S}^{(i)}[1, 1], k = 1, \dots, \min(K, c_{out}), \gamma \in [0, 1] \}| \quad (2)$$

²To clarify, this depth refers to the depth of the network. The *depthwise* in DeCEF refers to the depth (i.e. input channels) of a layer, which is a different concept.

where $|\cdot|$ denotes the cardinality of a set and $\mathbf{S}[k, k]$ is the k^{th} diagonal element of matrix \mathbf{S} .

- The effective rank of one layer l :

$$r^l = |\{s^l : s^l \geq \gamma, k = 1, \dots, \min(K, c_{out}), \gamma \in [0, 1]\}| \quad (3)$$

where $s^l = \mathbb{E}_i \left(\frac{\mathbf{S}^{(i)}[k, k]}{\mathbf{S}^{(i)}[1, 1]} \right)$ and the expected value can be estimated by averaging over all input channels i .

To illustrate the empirical values, examples can be found in Fig. [1]. and Fig. [2] in the supplementary material.

To summarize what we have observed:

- 1) the vectorized Conv2D filters in a trained CNN exhibit low rank properties (cf. Fig. [1] in supplementary);
- 2) the effective ranks of vectorized filters show a decreasing tendency when the network goes deeper (cf. Fig. [2] in supplementary);
- 3) the effective ranks of vectorized filters converge over training steps (see video in supplementary material).

Given these observations, we propose a new layer called DeCEF as an alternative parameterization to Conv2D layers for the purpose of reducing the redundancy.

2.2 Definition

In this section, we introduce the definition of DeCEF followed by its two properties. Generally speaking, subspace techniques bring better robustness to the learning system due to their reduced model complexity. Motivated by these observations and analyses, we define a DeCEF layer as follows.

Definition 2 (DeCEF layer). A DeCEF layer is defined by

$$\Theta = \left\{ \mathbf{w}_j^{(i)}, \mathbf{w}_j^{(i)} \in \mathbb{R}^{h \times h}, i = 1 \dots c_{in}, j = 1 \dots c_{out} \right\}$$

with the following parameterization

$$\mathbf{w}_j^{(i)} = \sum_{k=1}^r a_{k,j}^{(i)} \mathbf{u}_k^{(i)}, r \in [1, h^2] \quad (4)$$

where $a_{k,j}^{(i)} \in \mathbb{R}$ and $\mathbf{u}_k^{(i)} \in \mathbb{R}^{h \times h}$, which satisfies

$$\bar{\mathbf{u}}_l^{(i)T} \bar{\mathbf{u}}_m^{(i)} = \begin{cases} 1 & \text{if } l = m \\ 0 & \text{otherwise} \end{cases}$$

for $\bar{\mathbf{u}}_k^{(i)} = \text{vec}(\mathbf{u}_k^{(i)}) \in \mathbb{R}^{h^2}$. The parameters $\mathbf{u}_k^{(i)} \in \mathbb{R}^{h \times h}$ are called the **eigen-filters**.

Note that for the sake of clarity, we use Θ to denote the DeCEF layer, instead of the generic notation \mathcal{W} in Def.1.

2.3 Properties

In this section, we present two key properties of the DeCEF layer. These properties are then empirically evaluated in the experiment section.

Property 1. *Complexity (one layer)*

- *Number of trainable parameters (N)*
 - $N(\text{Conv2D})$: $c_{in}c_{out}h^2$
 - $N(\text{DeCEF})$: $N_u + N_a$, where
 - *Eigen-filters*: $N_u = c_{in}h^2r$
 - *Coefficients*: $N_a = c_{in}c_{out}r$

For $r = h^2$, it is trivial to randomly initialize eigen-filters that span the whole h^2 dimensional vector space and hence the eigen-filters do not need to be trainable, i.e. $N_u = 0$ and $N_a = c_{in}c_{out}h^2$. Therefore, Conv2D and DeCEF are equivalent for $r = h^2$.

For $r < h^2$, $N(\text{DeCEF}) < N(\text{Conv2D})$ if $r \leq \left\lfloor \frac{c_{out}h^2}{c_{out}+h^2} \right\rfloor$.

Example. Given $c_{in} = c_{out} = 128$ and $h = 3$, we have $N(\text{Conv2D}) = 147456$. If $r \leq 8 < h^2 = 9$, then $N(\text{DeCEF}) < N(\text{Conv2D})$. For $r = 8$, $N(\text{DeCEF}) = 140288$ and for $r = 4$, $N(\text{DeCEF}) = 70144$.

- *FLOPs (F)*

We count the multiply-accumulate operations (macc) and we do not include bias in our calculations. Given the dimension of the input layer $H \times W \times c_{in}$, let $t = \left\lfloor \frac{H}{\text{stride}} \right\rfloor \times \left\lfloor \frac{W}{\text{stride}} \right\rfloor$,

- $F(\text{Conv2D})$: $th^2c_{in}c_{out}$
- $F(\text{DeCEF})$: $tc_{in}r(h^2 + c_{out})$

Example. Given $H = W = 100$, $c_{in} = 128$, $c_{out} = 128$ and $h = 3$ with $\text{stride} = 1$, we have $F(\text{Conv2D}) = 1.47$ GFLOPs. For $r = 8$, $F(\text{DeCEF}) = 1.40$ GFLOPs. For $r = 4$, $F(\text{DeCEF}) = 0.70$ GFLOPs.

Property 2. *Robustness*

Lemma 1. Let $\Delta \mathbf{I}_i$ be an additive perturbation matrix and $\mathbf{w}_j^{(i)} \in \mathbb{R}^{h \times h}$ be a filter parameterized by Eq. (4), which is learned from some training process. Let

$$\bar{\mathbf{U}}^{(i)} = [\bar{\mathbf{u}}_0^{(i)}, \dots, \bar{\mathbf{u}}_r^{(i)}]. \quad (5)$$

If $\bar{\mathbf{U}}^{(i)T} \bar{\mathbf{U}}^{(i)} = \mathbf{I}$ and $\left\| \mathbf{a}_j^{(i)} \right\|_2 \leq \epsilon, \forall i, j$,

$$\left\| \sum_i \Delta \mathbf{I}_i * \mathbf{w}_j^{(i)} \right\|_\infty \leq \epsilon hr \sum_i \|\Delta \mathbf{I}_i\|_2. \quad (6)$$

Proof. See supplementary material. □

Robustness in this context is indicated by the propagation of the additive perturbation between input and output feature maps. Lemma 1 shows that when (1) $\bar{\mathbf{U}}^{(i)\text{T}}\bar{\mathbf{U}}^{(i)} = \mathbf{I}$, i.e. the vectorized filters are orthonormal, and (2) $\left\|\mathbf{a}_j^{(i)}\right\|_2 \leq \epsilon$, i.e. the coefficients are bounded by ϵ , the effect of the perturbation on the output is bounded by Eq. (6).

The rank r of the eigen-filters is a hyperparameter that yields a trade-off between the robustness and the representational power of a DeCEF layer. In this work, we use a rule based approach for choosing this hyperparameter.

2.4 Training algorithms

In this section, we show how to construct and train a network composed of DeCEF layers.

2.4.1 The optimization problem

Given a network architecture with a set of layers $\mathcal{N} = \{\mathcal{W}_1 \cdots \mathcal{W}_L\}$. Denote the index set of the network \mathcal{N} using $\mathcal{I}_{\mathcal{N}} = \{1, \cdots, L\}$. Let $\mathcal{G} = \{\Theta_{m_1} \cdots \Theta_{m_S}\} \subseteq \mathcal{N}$ be a set of DeCEF layers with index set $\mathcal{I}_{\mathcal{G}} = \{m_1, \cdots, m_S\}$. Let $\tilde{\mathcal{G}} = \mathcal{N} \setminus \mathcal{G}$ be the rest of the layers in the network. Let $f(\mathcal{N})$ be an objective function and $\lambda\Phi(\tilde{\mathcal{G}})$ be a regularization term applied to the set $\tilde{\mathcal{G}}$, where $\lambda > 0$ is the multiplier. The optimization problem is formulated as:

$$\begin{aligned} \min \quad & f(\mathcal{N}) + \lambda\Phi(\tilde{\mathcal{G}}) \\ \text{subject to} \quad & \bar{\mathbf{U}}_l^{(i)\text{T}}\bar{\mathbf{U}}_l^{(i)} = \mathbf{I} \\ & \left\|\mathbf{a}_{l,j}^{(i)}\right\|_2 \leq \epsilon, \forall l \in \mathcal{I}_{\mathcal{G}} \end{aligned} \quad (7)$$

2.4.2 Relaxed regularization

Finding an exact optimal DeCEF layer is an NP-hard problem due to the orthonormality constraint. Therefore, we approximate the constraint by the following regularizations. For a given DeCEF layer l , we have:

$$\Phi_1 : \quad \lambda_1 \left\|\bar{\mathbf{U}}^{(i)\text{T}}\bar{\mathbf{U}}^{(i)} - \mathbf{I}\right\|_2 \quad (8)$$

$$\Phi_2 : \quad \lambda_2 \left\|\mathbf{a}_j^{(i)}\right\|_2, \quad \mathbf{a}_j^{(i)} = [a_{1,j}^{(i)}, \cdots, a_{r,j}^{(i)}] \quad (9)$$

Note that the layer index l is neglected.

The loss function of the whole network is then written as:

$$f(\mathcal{N}) + \lambda\Phi(\tilde{\mathcal{G}}) + \lambda_1\Phi_1(\mathcal{G}) + \lambda_2\Phi_2(\mathcal{G}) \quad (10)$$

where $\Phi_i(\mathcal{G}) = \sum_{l \in \mathcal{I}_{\mathcal{G}}} \Phi_i^l$, $i = 1, 2$.

2.4.3 Deterministic rule-based hyperparameters

Hyperparameters are chosen based on deterministic rules to avoid complex hyperparameter tuning and to increase reproducibility. These rules are determined using a transfer

learning approach. First, we find the hyperparameters in DeCEF using cross-validation on a small dataset CIFAR-10, where cross-validation is affordable. Then we establish a deterministic rule for each hyperparameter. These rules are then directly applied to the larger dataset ImageNet without tuning. There are three sets of hyperparameters $h1 \sim h3$:

h1: Ranks r (Algo. 1): The observation of singular values from several networks shows that the effective ranks typically have a decreasing trend with respect to the depth, i.e., layers at the beginning of the network often have higher rank, and vice versa. The idea of choosing the rank before training a network is to find a monotonically decreasing function given the increasing depth. In this paper, we adopt two alternative routines for choosing the rank in each layer: linear decay (simple) and logarithmic decay (aggressive). Let l be the depth index of a layer and $K = h^2$. Denote $l_{\max} = \max(l)$ and $l_{\min} = \min(l)$.

- Linear decay: $\hat{r}_i = \left\lfloor K - \frac{l(K-1)}{l_{\max}-l_{\min}} \right\rfloor$.
- Logarithmic decay: $\hat{r}_i = \left\lfloor \frac{K-1}{\log_2(l+1)} \right\rfloor$.

h2: Regularization coefficients (Algo.1, cf. Eq. (8), (9)): $\lambda_1 = 0.0001r$ and $\lambda_2 = 0.0001$.

h3: Singular value threshold to determine the effective rank (cf. Eq. (2), (3)): $\gamma = 0.3$.

The training algorithm is summarized in Alg. 1.

Algorithm 1. (*DeCEF training strategy*)

- **Step 1:** Choose a network topology fully or partially composed of DeCEF layers. For example, one can replace all Conv2D layers with DeCEF layers.
- **Step 2:** Choose hyperparameters r, λ_1, λ_2 .
- **Step 3:** Initialization for each DeCEF layer ($k = 1, \dots, r$):

- Eigen-filters $\mathbf{u}_k^{(i)}$:
 - Generate random matrices: $\mathbf{A}^{(i)} \in \mathbb{R}^{K \times r}$.
 - Compute the truncated SVD: $\mathbf{A}^{(i)} = \bar{\mathbf{U}}^{(i)} \bar{\mathbf{S}}^{(i)} \bar{\mathbf{V}}^{(i)T}$.
 - Reshape each column in $\bar{\mathbf{U}}^{(i)}$ into matrix $\mathbf{u}_k^{(i)} \in \mathbb{R}^K$.
- Coefficients $a_{k,j}^{(i)}$: randomly initialized from a normal distribution.

Step 4: Forward and backward paths:

- Forward $\mathbf{I}_l \rightarrow \mathbf{I}_{l+1}$: for each out channel j ,

$$\mathbf{I}_{l+1}^j = \sum_{i=1}^{c_m} \sum_{k=1}^r a_{k,j}^{(i),l} \mathbf{u}_k^{(i),l} * \mathbf{I}_l^i$$

- Backward: backpropagation with the loss function described in Eq. (10).

2.5 Refactor a Conv2D network into DeCEF

There are such use cases where a pre-trained CNN is available and one needs to reduce the runtime complexity of the network. This is not the focus of this work but we also propose a compression algorithm presented in the supplementary material.

3 Related Work

To compare to the state-of-the-art techniques, in this section, we list the following existing approaches. More related work can be found in the supplementary material.

Subspace techniques: The first category is the Low-Rank Approximation (LRA) technique. There are mainly two different approaches in the existing literature: 1) *Separable bases:* Jaderberg et al. [29] decomposes the $d \times d$ filters into $1 \times d$ and $d \times 1$ filters to construct rank-1 bases in the spatial domain. In later work [52][35], closed form solutions that significantly improves the efficiency over previous iterative optimization solvers are proposed. Ioannou et al. [28] introduces a novel weight initialization that allows small basis filters to be trained from scratch, which has achieved similar or higher accuracy than the conventional CNNs. Yu et al. [60] proposes a SVD-free algorithm that uses the idea that filters usually share smooth components in a low-rank subspace. Alvarez and Salzmann [2] introduces a regularizer that encourages the weights of the layers to have low rank during the training. 2) *Filter vectorization:* Some existing work implements the low rank approximation by vectorizing the filters. For instance, Denton et al. [8] stacks all filters for each output channel into a high dimensional vector space and approximates the trained filters using SVD. Wen et al. [56] presents a regularization to enforce filters to coordinate into lower-rank space, where the subspaces are constructed from all the input channels for each given output channel. Recently, Peng et al. [47] proposed a decomposition focusing on exploiting the filter group structure for each layer.

Pruning: Pruning refers to techniques that aim at reducing the number of parameters in a pre-trained network by identifying and removing redundant weights. This is a very invested topic in the attempt to reduce the model complexity. Although being different from our use case, we list the state-of-the-art pruning techniques in this section to have a more complete view on model reduction techniques. In *Optimal Brain Damage* by LeCun et al. [32], and later in *Optimal Brain Surgeon* by Hassibi et al. [15], redundant weights are defined by their impact on the objective function, which are identified using the Hessian of the loss function. Other definitions of redundancy have been proposed in subsequent work. For instance, Anwar et al. [3] applies pruning on the filter-level of CNNs by using particle filters to propose pruning candidates. Han et al. [14] introduces a simpler pruning method using a strong L2 regularization term, where weights under a certain threshold are removed. Molchanov et al. [45] uses Taylor expansion to approximate the influence in the loss function by removing each filter. Hu et al. [23] iteratively optimizes the network by pruning unimportant neurons based on analysis of their outputs on a large dataset. Li et al. [33] identifies and removes filters having a small effect on the accuracy. Aghasi et al. [1] prunes a trained network layer-wise by solving a convex optimization program. Liu et al. [41] takes wide and large networks as input models, but during training insignificant channels are automatically identified and pruned afterwards. More recently, in [42] and [44], Luo et al. analyzes the redundancy of filters in a trained network by looking at statistics computed from its next layer. He et al. [21] proposes an iterative LASSO regression based channel selection algorithm.

Huang et al. [25] removes filters by training a pruning agent to make decisions for a given reward function. In [59], Yu et al. poses the pruning problem as a binary integer optimization and derives a closed-form solution based on final response importance. Lin et al. [36] prunes filters across all layers by proposing a global discriminative function based on prior knowledge of each filter. Tung and Mori [54] combines network pruning and weight quantization in a single learning framework that performs pruning and quantization jointly. Zhang et al. [61] first formulate the weight pruning problem as a nonconvex optimization problem constraints specifying the sparsity requirements and optimize using the alternating direction method of multipliers. Other work [62] uses discrimination-aware losses into the network to increase the discriminative power of intermediate layers. [26] adds a scaling factor to the outputs and then add sparsity regularizations on these factors. He et al. [19] compresses CNN models by pruning filters with redundancy, rather than those with "relatively less" importance. Lin et al. [37] proposes a scheme that incorporates two different regularizers which fully coordinates the global output and local pruning operations to adaptively prune filters. Later, Lin et al. [38], proposed an effective structured pruning approach that jointly prunes filters as well as other structures in an end-to-end manner by defining a new objective function with sparsity regularization which is solved by generative adversarial learning. Ding et al. [9] proposes a novel optimization method, which can train several filters to collapse into a single point in the parameter hyperspace which can be trimmed with no performance loss. Liu et al. [40] proposes a meta network, which is able to generate weight parameters for any pruned structure given the target network, which can be used to search for good-performing pruned networks. [58] introduce gate decorators to identify unimportant filters to prune. [46] prunes filters by using Taylor expansions to approximate a filter's contribution. [10] finds the least important filters to prune by a binary search. which keeps searching for the least important filters in a binary search manner Luo and Wu [43] proposes an efficient channel selection layer to find less important filters automatically in a joint training manner. Lin et al. [34] proposes a method that is mathematically formulated to prune filters with low-rank feature maps. [20] introduces a differentiable pruning criteria sampler. [11] proposes a re-parameterization of CNNs to a remembering part and a forgetting part. The former learns to maintain the performance and the latter learns for efficiency. [39] proposes a layer grouping algorithm to find coupled channels automatically. [50] uses an effective estimation of each filter, i.e., saliency, to measured filters from two aspects: the importance for prediction performance and the consumed computational resources. This can be used to preserve the prediction performance while zeroing out more computation-heavy filters.

Architectural design: Effort has been put into designing a smaller network architecture without loss of the generalization ability. For instance, He et al. [16] achieves a higher accuracy in [16, 17] compared to other more complex networks by introducing the residual building block. The residual building blocks adds an identity mapping that allows the signals to be directly propagated between the layers. Iandola et al. [27] introduces SqueezeNet and the Fire module, which is designed to reduce the number of parameters in a network by introducing 1×1 filters. By utilizing dense connections pattern between blocks, Huang et al. [24] manages to reduce the number of required parameters. Xie et al. [57] proposed a multi-branch architecture which exposes a new hyperparameter for each block to control the capacity of the network. Other work, like MobileNet[22, 49] and EfficientNet[53] specifically focus on building architectures suitable for devices with low compute capacity, such as mobile phones. By a design that maintains a high-resolution representation throughout the whole network, Wang

et al. [55] achieves good accuracy and performance in HRNet.

Compression: Deep Compression, by Han et al. [13], reduces the storage size of the model using quantization and Huffman encoding to compress the weights in the network. Other work on reducing the memory size of models is done by binarization. In XNOR-Net by Rastegari et al. [48], the weights are reduced to a binary representation and convolutions are replaced by XNOR operations. More recently, Suau et al. [51] proposed to analyze filter responses to automatically select compression methods for each layer.

Weight sharing: Another approach to reduce the number of parameters in a network is to share weights between the filters and layers. Boulch [5] share weights between the layers in a residual network operating on the same scale.

Depthwise separable convolutions: introduced by Chollet [6], have shown to be a more efficient use of parameters compared to regular Conv2Ds Inception like architectures. Depthwise separable convolutions have also been used in other work, e.g., in [21] by He et al., where it was used to gain a computational speed-up of ResNet networks.

Our focus: We observe and analyze the Conv2D from a different perspective compared to the previous subspace techniques. More specifically, i) we vectorize the filters instead of using separable basis in the original vector space (Jaderberg et al. [29], Tai et al. [52], Ioannou et al. [28], Yu et al. [60]); ii) we do not concatenate these vectorized filters into a large vector space (Denton et al. [8], Wen et al. [56], Peng et al. [47]), which achieves a better modularity compared to the concatenated vectors. Our perspective is motivated by the empirical evidence from our experiments. This opens up new opportunities and provides new analytical tools for understanding the design of convolutional networks with respect to their subspace redundancies. In our experiments, we choose a popular base network (ResNet) and compare our experimental results to various modifications of the same base network. We also conduct tests on other more recent network architectures such as HRNet-W18-C and DenseNet-121 for further comparison and validation.

4 Experiments and Results

4.1 Hardware

For training and experiments, Nvidia Tesla V100 SXM2 with 32 GB of GPU memory are used.

4.2 Dataset CIFAR-10: Ablation Study

Dataset: To empirically study the behavior of DeCEF, we conduct various experiments on the standard image recognition dataset CIFAR-10 by Krizhevsky and Hinton [31].

Benchmark: We use ResNet-32 as the base net for comparison. ResNet-32 has three **blocks**, where the last block (block-3) in ResNet-32 has the most filters. Since our goal is to reduce the amount of trainable parameters and FLOPs, we mainly vary the structure in block-3 in our experiments.

Experiments: We design four experiments as follows.

Experiment 1. Varying rank r and c_{out} For a layer with input channels $i = 1, \dots, c_{\text{in}}$ and output channels $j = 1, \dots, c_{\text{out}}$, the filters in the DeCEF layer is expressed as

$\mathbf{w}_j^{(i)} = \sum_{k=1}^r a_{k,j}^{(i)} \mathbf{u}_k^{(i)}$. We empirically show that DeCEF layers achieve higher accuracy with significantly lower number of parameters. In this experiment, we vary two hyperparameters: 1) the rank r of each filter in the DeCEF layer, and 2) the number of output channels c_{out} . We compare the accuracy versus the number of parameters in different types of layers (Conv2D and DeCEF with different hyperparameters). As shown in Fig. 1, with a lower number of parameters, DeCEF achieves a better accuracy with low rank techniques. Moreover, when we increase the number of output channels, DeCEF shows a even more promising result with fewer parameters in total.

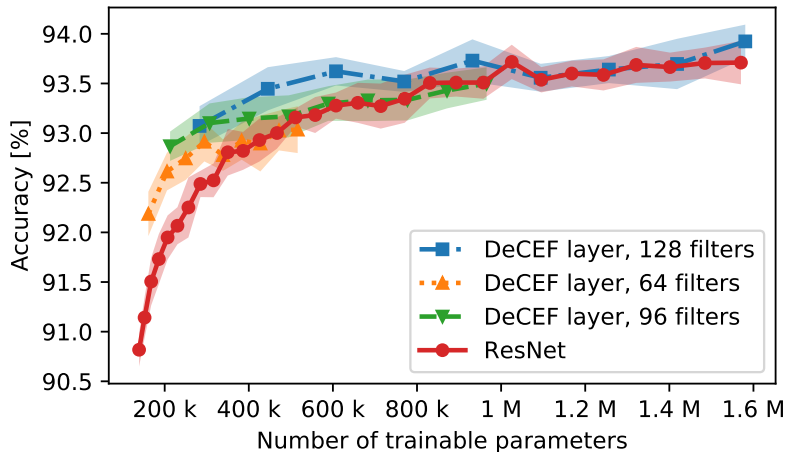


Figure 1: Accuracy versus number of parameters on CIFAR-10.

Experiment 2. Trainable vs frozen eigen-filters In Algo. 1, the eigen-filters in DeCEF layers are trained simultaneously using backpropagation. In this experiment, we investigate the impact of this training process and try to understand if it is sufficient to use *random basis vectors* as eigen-filters. We initialize the eigen-filters according to Algo. 1 and freeze them during training. The comparison between the accuracies achieved by frozen and trainable eigen-filters can be found in Fig. 2. By using frozen eigen-filters, the network has a fewer number of trainable parameters for the same rank. With a low rank ($r < 5$), the accuracy is degraded without training.

Experiment 3. With or without Φ_1 regularization To study the effect of Φ_1 introduced in Eq. (8), some experiments can be found in Fig. 2. We can see that with a high rank, the regularization needs to be applied. In our experiment, we use $\lambda_1 = 0.0001r$ and $\lambda_2 = 0.0001$, where λ_1 is the multiplier of the constraint on the eigen-filters and λ_2 is on the subspace coefficients. The reason for having the multiplier r in λ_1 is to suppress the growth of the cost when r becomes large.

Experiment 4. Comparison to related work In this experiment, we implement Algo. 1 (DeCEF-ResNet-32) to compared to the state-of-the-art techniques. We vary

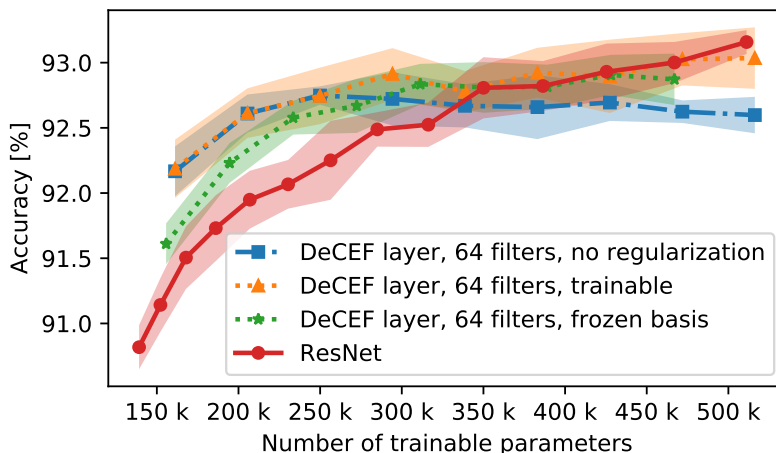


Figure 2: DeCEF layer with trainable vs frozen bases on CIFAR-10.

the number of output channels c_{out} in the last ResNet block for comparison, where we see that having fewer eigen-filters with more output channels yields a better result.

Results: The results are presented in terms of the estimated mean and the standard deviation of the classification accuracy on the testing set with 10 runs for each experimental setup, which are shown in Fig. 1 and Fig. 2. The accuracy is then presented with respect to the number of trainable parameters for each network structure. For DeCEF layers, there are nine data points in each presented result, which correspond to different layer ranks in block-3 $r_3 \in \{1, \dots, 9\}$. In addition, the number of trainable parameters in DeCEF layers is also varied by using different numbers of output channels in block-3, i.e., $c_{\text{out}} \in \{64, 96, 128\}$. We then vary c_{out} in ResNet-32 block-3 ($c_{\text{out}} \in \{16, 20, 24, \dots, 128\}$) to have a comparable result. We compare the accuracy achieved by DeCEF-ResNet-32 Fig. 3. Additional results can be found in the supplementary material.

4.3 Dataset ImageNet (ILSVRC-2012)

4.3.1 Accuracy versus complexity

To further compare our algorithms to the state-of-the-art, we use the standard dataset ImageNet (ILSVRC-2012) by Deng et al. [7]. ImageNet has 1.2 M training images and 50 k validation images of 1000 object classes, commonly evaluated by Top-1 and Top-5 accuracy. We use the networks ResNet-50 v2 He et al. [17], DenseNet-121 Huang et al. [24] and HRNet-W18-C Wang et al. [55] as the base networks. The results are visualized in Fig. 4 for Top-1 accuracy (Top-5 accuracy can be found in the supplementary material).

The hyperparameters used in DeCEF-ResNet-50 are determined by the deterministic rules presented in **h1**, **h2** and **h3**. For each setup, we have five runs and report the average accuracy and its standard deviation in the supplementary material. From the experiments, we see the trade-off between the two rank decay mechanisms: linear decay

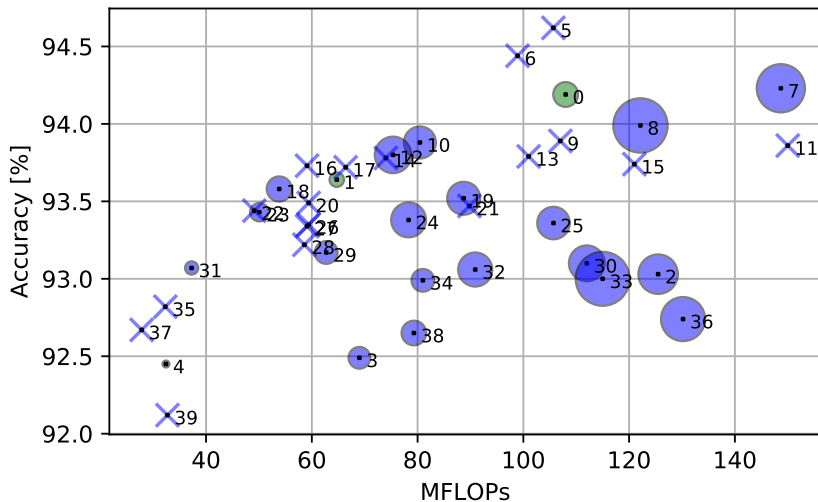


Figure 3: Ball chart for CIFAR-10, where the size of the ball indicates the number of trainable parameters. For papers that have not reported the FLOPs, we use a cross instead of a ball to represent them. The exact values are reported in Table 1. The number in each ball is the network ID, which is indicated as the superscript of each entry in Table 1.

is less aggressive, which yield to a better accuracy, whereas logarithmic decay reduce a greater number of FLOPs while still having a decent accuracy. To further validate DeCEF, we run the same experiments on three commonly used base networks. The results are reported in Tab. 2 and Tab. 3 to compare with the corresponding base network and state-of-the-art model reduction techniques.

4.4 Limitation

This work focuses on the model reduction aspect given the observations of the low rank behaviors. The analysis of these behaviors needs to be further explored as a future direction, which brings the limitation that the rules for choosing the hyperparameters are rather heuristic.

5 Conclusion and future work

In this paper, we propose a new methodology to observe and analyze the redundancy in a CNN. Motivated by our observations of the low rank behaviors in vectorized Conv2D filters, we present a layer structure DeCEF as an alternative parameterization to Conv2D filters for the purpose of reducing their complexity in terms of trainable parameters and FLOPs. Our experiments have shown that in a convolutional layer with filter size

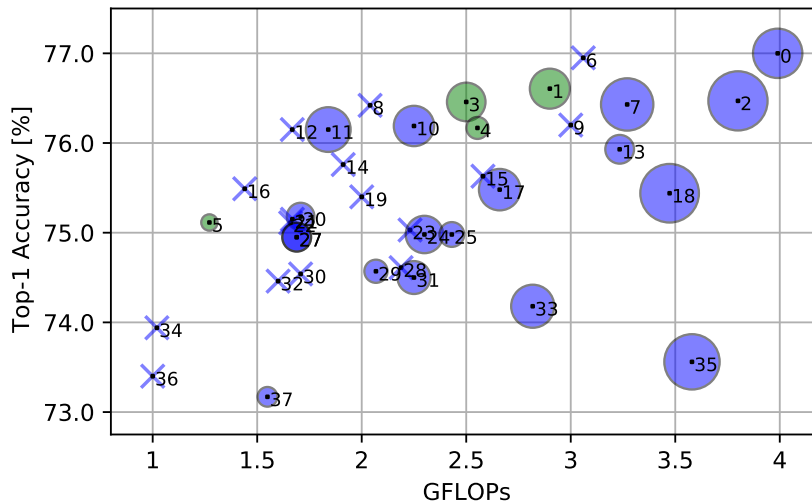


Figure 4: Ball chart for ImageNet Top-1 accuracy with the same set up as Fig. 3. The corresponding values can be found in Table 3.

$h \times h$, it is not necessary to have more than h^2 eigen-filters given the training strategy in Sec. 2.4.

In terms of the accuracy-to-complexity ratio, it is beneficial to use more coefficients (i.e. output channels) with fewer eigen-filters in DeCEF layers. The DeCEF layer is simple to implement in most deep learning frameworks using depthwise separable convolutions with a new training strategy. With the deterministic rules for choosing hyperparameters, it is easy to design and reproduce the results. From our observations, the underlying subspace structure is a commonly shared property among different network architectures and topologies, which provides insights to the design and analysis of CNNs.

As future directions, first we will further analyze this low rank structure to improve rank decay functions by designing more sophisticated strategies. For instance, in some network architectures, the effective rank first increases and then quickly decreases with respect to the depth. This is a phenomenon that we would like to study further. Moreover, since the DeCEF layer can be implemented by the depthwise separable convolutions with a new training strategy, a second future direction is to modify and train the traditional depthwise separable convolutional layers in well-known networks using DeCEF to reduce the model complexity. Finally, during the experiments, we have come up with several hypotheses regarding the low rank behaviors in deep neural networks, which we plan to explore to better understand and interpret a CNN from this perspective.

Network	Acc.	No. param.	MFLOPs
(a) DeCEF vs baseline network			
DeCEF-ResNet-32 (32, 64, 128) ⁰	94.19 %	533.00 k	108.00
DeCEF-ResNet-32 (24, 48, 96) ¹	93.64 %	311.00 k	64.72
ResNet-56 ² [16]	93.03 %	850.00 k	125.49
ResNet-32 ³ [16]	92.49 %	467.00 k	69.00
DeCEF-ResNet-32 (16, 32, 64) ⁴	92.45 %	148.00 k	32.42
(b) Related work			
ResRep ResNet-110 ⁵ [11]	94.62 %		105.68
C-SGD-5/8 ResNet-110 ⁶ [9]	94.44 %		98.91
HRank ResNet-110 1 ⁷ [34]	94.23 %	1.04 M	148.70
SASL ResNet-110 ⁸ [50]	93.99 %	1.17 M	122.15
SFP ResNet-56 10% ⁹ [18]	93.89 %		107.00
SASL ResNet-56 ¹⁰ [50]	93.88 %	689.35 k	80.44
SFP ResNet-110 30% ¹¹ [18]	93.86 %		150.00
SASL* ResNet-110 ¹² [50]	93.80 %	786.04 k	75.36
LFPC ResNet-110 ¹³ [20]	93.79 %		101.00
SFP ResNet-56 30% ¹⁴ [18]	93.78 %		74.00
FPGM-only 40% ResNet-110 ¹⁵ [19]	93.74 %		121.00
ResRep ResNet-56 1 ¹⁶ [11]	93.73 %		59.09
LFPC ResNet-56 1 ¹⁷ [20]	93.72 %		66.40
SASL* ResNet-56 ¹⁸ [50]	93.58 %	538.90 k	53.84
HRank ResNet-56 1 ¹⁹ [34]	93.52 %	710.00 k	88.72
FPGM-only 40% ResNet-56 ²⁰ [19]	93.49 %		59.40
SFP ResNet-56 20% ²¹ [18]	93.47 %		89.80
C-SGD-5/8 ResNet-56 ²² [9]	93.44 %		49.13
GBN-40 ²³ [58]	93.43 %	395.25 k	50.07
GAL-0.6 ResNet-56 ²⁴ [38]	93.38 %	750.00 k	78.30
HRank ResNet-110 2 ²⁵ [34]	93.36 %	700.00 k	105.70
SFP ResNet-56 40% ²⁶ [18]	93.35 %		59.40
LFPC ResNet-56 2 ²⁷ [20]	93.34 %		59.10
SFP ResNet-32 10% ²⁸ [18]	93.22 %		58.60
HRank ResNet-56 2 ²⁹ [34]	93.17 %	490.00 k	62.72
ResNet-56-pruned-A ³⁰ [33]	93.10 %	770.10 k	112.00
GBN-30 ³¹ [58]	93.07 %	283.05 k	37.27
ResNet-56-pruned-B ³² [33]	93.06 %	733.55 k	90.90
ResNet-110-pruned-B ³³ [33]	93.00 %	1.16 M	115.00
NISP-56 ³⁴ [59]	92.99 %	487.90 k	81.00
FPGM-mix 40% ResNet-32 ³⁵ [19]	92.82 %		32.30
GAL-0.5 ResNet-110 ³⁶ [38]	92.74 %	950.00 k	130.20
ResRep ResNet-56 2 ³⁷ [11]	92.67 %		27.82
HRank ResNet-110 3 ³⁸ [34]	92.65 %	530.00 k	79.30
LFPC ResNet-32 ³⁹ [20]	92.12 %		32.70

Table 1: Comparison to state-of-the-art model reduction techniques on CIFAR-10.

	layers	rank decay	Top-1	Top-5	params	(G)FLOPs
ResNet-50	Conv2D	None	76.47 %	93.21%	25.56M	3.80
	DeCEF	Linear	76.61%	93.22%	17.27M	2.90
	DeCEF	Logarithmic	76.46%	93.24%	16.64M	2.50
DenseNet-121	Conv2D	None	74.81%	92.32%	79.79M	2.83
	DeCEF	Linear	74.85%	92.61%	72.10M	2.81
	DeCEF	Logarithmic	74.40%	91.89%	62.92M	2.11
HRNet-W18-C	Conv2D	None	77.00%	93.50%	21.30M	3.99
	DeCEF	Linear	76.17%	92.99%	9.490M	2.55
	DeCEF	Logarithmic	75.11%	92.47%	7.05M	1.27

Table 2: Comparison to the base networks on ImageNet.

Network	Top-5 Acc.	Top-1 Acc.	No. param.	GFLOPs
(a) DeCEF vs baseline network				
HRNet-W18-C ⁰ [55]	93.50 %	77.00 %	21.30 M	3.99
DeCEF-ResNet-50 (lin decay) ¹	93.22 %	76.61 %	17.27 M	2.90
ResNet-50 ² [17]	93.21 %	76.47 %	25.56 M	3.80
DeCEF-ResNet-50 (log decay) ³	93.24 %	76.46 %	16.64 M	2.50
DeCEF-HRNet-W18-C (lin decay) ⁴	92.99 %	76.17 %	9.49 M	2.55
DeCEF-HRNet-W18-C (log decay) ⁵	92.47 %	75.11 %	7.05 M	1.27
(b) Related work				
GFP ResNet-50 1 ⁶ [39]		76.95 %		3.06
Taylor-FO-BN-91% ⁷ [46]		76.43 %	22.60 M	3.27
GFP ResNet-50 2 ⁸ [39]		76.42 %		2.04
MetaPruning 0.85 ResNet-50 ⁹ [40]		76.20 %		3.00
GBN-60 ¹⁰ [58]	92.83 %	76.19 %	17.42 M	2.25
ResNet-50 GAL-0.5-joint ¹¹ [38]	90.82 %	76.15 %	19.31 M	1.84
ResRep ResNet-50 1 ¹² [11]	92.90 %	76.15 %		1.67
SSS-ResNetXt-41 ¹³ [26]	93.00 %	75.93 %	12.40 M	3.23
SASL ¹⁴ [50]	92.82 %	75.76 %		1.91
AOFP-C1 ¹⁵ [10]	92.69 %	75.63 %		2.58
ResRep ResNet-50 2 ¹⁶ [11]	92.55 %	75.49 %		1.44
Taylor-FO-BN-81% ¹⁷ [46]		75.48 %	17.90 M	2.66
SSS-ResNet-41 ¹⁸ [26]	92.61 %	75.44 %	25.30 M	3.47
MetaPruning 0.75 ResNet-50 ¹⁹ [40]		75.40 %		2.00
GBN-50 ²⁰ [58]	92.41 %	75.18 %	11.91 M	1.71
SASL* ²¹ [50]	92.47 %	75.15 %		1.67
AOFP-C2 ²² [10]	92.28 %	75.11 %		1.66
ResNet-50 FPGM-only 30% ²³ [19]	92.40 %	75.03 %		2.23
ResNet-50 HRank 1 ²⁴ [34]	92.33 %	74.98 %	16.15 M	2.30
SSS-ResNetXt-38 ²⁵ [26]	92.50 %	74.98 %	10.70 M	2.43
DCP ²⁶ [62]	92.32 %	74.95 %	12.41 M	1.69
DCP ²⁷ [62]	92.32 %	74.95 %	12.41 M	1.69
SFP ²⁸ [18]	92.06 %	74.61 %		2.19
SSS-ResNetXt-35-A ²⁹ [26]	92.17 %	74.57 %	10.00 M	2.07
C-SGD-50 ³⁰ [9]	92.09 %	74.54 %		1.71
Taylor-FO-BN-72% ³¹ [46]		74.50 %	14.20 M	2.25
LFPC ³² [20]	92.04 %	74.46 %		1.60
SSS-ResNet-32 ³³ [26]	91.91 %	74.18 %	18.60 M	2.82
GFP ResNet-50 3 ³⁴ [39]		73.94 %		1.02
Pruned-90 ³⁵ [42]	91.60 %	73.56 %	23.89 M	3.58
MetaPruning 0.5 ResNet-50 ³⁶ [40]		73.40 %		1.00
SSS-ResNetXt-35-B ³⁷ [26]	91.58 %	73.17 %	8.50 M	1.55

Table 3: Comparison to state-of-the-art model reduction techniques on ImageNet.

References

- [1] Alireza Aghasi, Afshin Abdi, Nam Nguyen, and Justin Romberg. Net-trim: Convex pruning of deep neural networks with performance guarantee. In *Advances in Neural Information Processing Systems*, pages 3177–3186, 2017.
- [2] Jose M Alvarez and Mathieu Salzmann. Compression-aware training of deep networks. In *Advances in Neural Information Processing Systems*, pages 856–867, 2017.
- [3] Sajid Anwar, Kyuyeon Hwang, and Wonyong Sung. Structured pruning of deep convolutional neural networks. *J. Emerg. Technol. Comput. Syst.*, 13(3):32:1–32:18, feb 2017. ISSN 1550-4832. doi: 10.1145/3005348.
- [4] P.N. Belhumeur, J.P. Hespanha, and D.J. Kriegman. Eigenfaces vs fisher faces recognition using class specific linear projection. *IEEE Transactions on Pattern Analysis and Machine Intelligence*, 19:711–720, 1997.
- [5] Alexandre Boulch. Reducing parameter number in residual networks by sharing weights. *Pattern Recognition Letters*, 103:53 – 59, 2018. ISSN 0167-8655. doi: <https://doi.org/10.1016/j.patrec.2018.01.006>.
- [6] Francois Chollet. Xception: Deep learning with depthwise separable convolutions. In *The IEEE Conference on Computer Vision and Pattern Recognition (CVPR)*, July 2017.
- [7] J. Deng, W. Dong, R. Socher, L. Li, Kai Li, and Li Fei-Fei. Imagenet: A large-scale hierarchical image database. In *2009 IEEE Conference on Computer Vision and Pattern Recognition*, pages 248–255, June 2009. doi: 10.1109/CVPR.2009.5206848.
- [8] Emily L Denton, Wojciech Zaremba, Joan Bruna, Yann LeCun, and Rob Fergus. Exploiting linear structure within convolutional networks for efficient evaluation. In Z. Ghahramani, M. Welling, C. Cortes, N. D. Lawrence, and K. Q. Weinberger, editors, *Advances in Neural Information Processing Systems 27*, pages 1269–1277. Curran Associates, Inc., 2014.
- [9] Xiaohan Ding, Guiguang Ding, Yuchen Guo, and Jungong Han. Centripetal sgd for pruning very deep convolutional networks with complicated structure. In *Proceedings of the IEEE Conference on Computer Vision and Pattern Recognition*, pages 4943–4953, 2019.
- [10] Xiaohan Ding, Guiguang Ding, Yuchen Guo, Jungong Han, and Chenggang Yan. Approximated oracle filter pruning for destructive CNN width optimization. In Kamalika Chaudhuri and Ruslan Salakhutdinov, editors, *Proceedings of the 36th International Conference on Machine Learning*, volume 97 of *Proceedings of Machine Learning Research*, pages 1607–1616. PMLR, 09–15 Jun 2019.
- [11] Xiaohan Ding, Tianxiang Hao, Ji Liu, Jungong Han, Yuchen Guo, and Guiguang Ding. Lossless cnn channel pruning via gradient resetting and convolutional re-parameterization. *arXiv preprint arXiv:2007.03260*, 1, 2020.
- [12] G. Golub and C. van Loan. *Matrix Computations, 3rd edition*. Johns Hopkins Press, 1996.

- [13] Song Han, Huizi Mao, and William J Dally. Deep compression: Compressing deep neural networks with pruning, trained quantization and huffman coding. *arXiv preprint arXiv:1510.00149*, 2015.
- [14] Song Han, Jeff Pool, John Tran, and William J. Dally. Learning both weights and connections for efficient neural networks. In *Proceedings of the 28th International Conference on Neural Information Processing Systems - Volume 1, NIPS'15*, pages 1135–1143, Cambridge, MA, USA, 2015. MIT Press.
- [15] B. Hassibi, D. G. Stork, and G. J. Wolff. Optimal brain surgeon and general network pruning. In *IEEE International Conference on Neural Networks*, pages 293–299 vol.1, 1993. doi: 10.1109/ICNN.1993.298572.
- [16] K. He, X. Zhang, S. Ren, and J. Sun. Deep residual learning for image recognition. In *2016 IEEE Conference on Computer Vision and Pattern Recognition (CVPR)*, pages 770–778, June 2016. doi: 10.1109/CVPR.2016.90.
- [17] Kaiming He, Xiangyu Zhang, Shaoqing Ren, and Jian Sun. Identity mappings in deep residual networks. In *European conference on computer vision*, pages 630–645. Springer, 2016.
- [18] Yang He, Guoliang Kang, Xuanyi Dong, Yanwei Fu, and Yi Yang. Soft filter pruning for accelerating deep convolutional neural networks. *arXiv preprint arXiv:1808.06866*, 2018.
- [19] Yang He, Ping Liu, Ziwei Wang, Zhilan Hu, and Yi Yang. Filter pruning via geometric median for deep convolutional neural networks acceleration. In *Proceedings of the IEEE Conference on Computer Vision and Pattern Recognition*, pages 4340–4349, 2019.
- [20] Yang He, Yuhang Ding, Ping Liu, Linchao Zhu, Hanwang Zhang, and Yi Yang. Learning filter pruning criteria for deep convolutional neural networks acceleration. In *Proceedings of the IEEE/CVF Conference on Computer Vision and Pattern Recognition (CVPR)*, June 2020.
- [21] Yihui He, Xiangyu Zhang, and Jian Sun. Channel Pruning for Accelerating Very Deep Neural Networks. *Proceedings of the IEEE International Conference on Computer Vision*, 2017-Octob:1398–1406, 2017. ISSN 15505499. doi: 10.1109/ICCV.2017.155.
- [22] Andrew G Howard, Menglong Zhu, Bo Chen, Dmitry Kalenichenko, Weijun Wang, Tobias Weyand, Marco Andreetto, and Hartwig Adam. Mobilenets: Efficient convolutional neural networks for mobile vision applications. *arXiv preprint arXiv:1704.04861*, 2017.
- [23] Hengyuan Hu, Rui Peng, Yu-Wing Tai, and Chi-Keung Tang. Network trimming: A data-driven neuron pruning approach towards efficient deep architectures. *arXiv preprint arXiv:1607.03250*, 2016.
- [24] Gao Huang, Zhuang Liu, Laurens van der Maaten, and Kilian Q. Weinberger. Densely connected convolutional networks, 2016.
- [25] Qiangui Huang, Kevin Zhou, Suya You, and Ulrich Neumann. Learning to prune filters in convolutional neural networks. *arXiv preprint arXiv:1801.07365*, 2018.

- [26] Zehao Huang and Naiyan Wang. Data-driven sparse structure selection for deep neural networks. In *Proceedings of the European conference on computer vision (ECCV)*, pages 304–320, 2018.
- [27] Forrest N Iandola, Song Han, Matthew W Moskewicz, Khalid Ashraf, William J Dally, and Kurt Keutzer. Squeezenet: Alexnet-level accuracy with 50x fewer parameters and 0.5 mb model size. *arXiv preprint arXiv:1602.07360*, 2016.
- [28] Yani Ioannou, Duncan Robertson, Jamie Shotton, Roberto Cipolla, and Antonio Criminisi. Training cnns with low-rank filters for efficient image classification. *arXiv preprint arXiv:1511.06744*, 2015.
- [29] Max Jaderberg, Andrea Vedaldi, and Andrew Zisserman. Speeding up convolutional neural networks with low rank expansions. In *Proceedings of the British Machine Vision Conference*. BMVA Press, 2014. doi: <http://dx.doi.org/10.5244/C.28.88>.
- [30] I. T. Jolliffe. Principal component analysis. *Springer-Verlag*, 1986.
- [31] Alex Krizhevsky and Geoffrey Hinton. Learning multiple layers of features from tiny images. Technical report, Citeseer, 2009.
- [32] Yann LeCun, John S. Denker, and Sara A. Solla. Optimal brain damage. In D. S. Touretzky, editor, *Advances in Neural Information Processing Systems 2*, pages 598–605. Morgan-Kaufmann, 1990.
- [33] Hao Li, Asim Kadav, Igor Durdanovic, Hanan Samet, and Hans Peter Graf. Pruning filters for efficient convnets. *arXiv preprint arXiv:1608.08710*, 2016.
- [34] Mingbao Lin, Rongrong Ji, Yan Wang, Yichen Zhang, Baochang Zhang, Yonghong Tian, and Ling Shao. Hrank: Filter pruning using high-rank feature map. In *Proceedings of the IEEE/CVF Conference on Computer Vision and Pattern Recognition*, pages 1529–1538, 2020.
- [35] Shaohui Lin, Rongrong Ji, Chao Chen, Dacheng Tao, and Jiebo Luo. Holistic cnn compression via low-rank decomposition with knowledge transfer. *IEEE transactions on pattern analysis and machine intelligence*, 41(12):2889–2905, 2018.
- [36] Shaohui Lin, Rongrong Ji, Yuchao Li, Yongjian Wu, Feiyue Huang, and Baochang Zhang. Accelerating convolutional networks via global & dynamic filter pruning. In *IJCAI*, pages 2425–2432, 2018.
- [37] Shaohui Lin, Rongrong Ji, Yuchao Li, Cheng Deng, and Xuelong Li. Toward compact convnets via structure-sparsity regularized filter pruning. *IEEE transactions on neural networks and learning systems*, 31(2):574–588, 2019.
- [38] Shaohui Lin, Rongrong Ji, Chenqian Yan, Baochang Zhang, Liujuan Cao, Qixiang Ye, Feiyue Huang, and David Doermann. Towards optimal structured cnn pruning via generative adversarial learning. In *Proceedings of the IEEE Conference on Computer Vision and Pattern Recognition*, pages 2790–2799, 2019.

- [39] Liyang Liu, Shilong Zhang, Zhanghui Kuang, Aojun Zhou, Jing-Hao Xue, Xinjiang Wang, Yimin Chen, Wenming Yang, Qingmin Liao, and Wayne Zhang. Group fisher pruning for practical network compression. In Marina Meila and Tong Zhang, editors, *Proceedings of the 38th International Conference on Machine Learning*, volume 139 of *Proceedings of Machine Learning Research*, pages 7021–7032. PMLR, 18–24 Jul 2021.
- [40] Zechun Liu, Haoyuan Mu, Xiangyu Zhang, Zichao Guo, Xin Yang, Kwang-Ting Cheng, and Jian Sun. Metapruning: Meta learning for automatic neural network channel pruning. In *Proceedings of the IEEE International Conference on Computer Vision*, pages 3296–3305, 2019.
- [41] Zhuang Liu, Jianguo Li, Zhiqiang Shen, Gao Huang, Shoumeng Yan, and Changshui Zhang. Learning efficient convolutional networks through network slimming. In *Proceedings of the IEEE International Conference on Computer Vision*, pages 2736–2744, 2017.
- [42] Jian-Hao Luo and Jianxin Wu. An entropy-based pruning method for cnn compression. *arXiv preprint arXiv:1706.05791*, 2017.
- [43] Jian-Hao Luo and Jianxin Wu. Autopruner: An end-to-end trainable filter pruning method for efficient deep model inference. *Pattern Recognition*, page 107461, 2020.
- [44] Jian-Hao Luo, Jianxin Wu, and Weiyao Lin. Thinet: A filter level pruning method for deep neural network compression. In *Proceedings of the IEEE international conference on computer vision*, pages 5058–5066, 2017.
- [45] Pavlo Molchanov, Stephen Tyree, Tero Karras, Timo Aila, and Jan Kautz. Pruning convolutional neural networks for resource efficient inference. *arXiv preprint arXiv:1611.06440*, 2016.
- [46] Pavlo Molchanov, Arun Mallya, Stephen Tyree, Iuri Frosio, and Jan Kautz. Importance estimation for neural network pruning. In *Proceedings of the IEEE/CVF Conference on Computer Vision and Pattern Recognition (CVPR)*, June 2019.
- [47] Bo Peng, Wenming Tan, Zheyang Li, Shun Zhang, Di Xie, and Shiliang Pu. Extreme network compression via filter group approximation. In *Proceedings of the European Conference on Computer Vision (ECCV)*, pages 300–316, 2018.
- [48] Mohammad Rastegari, Vicente Ordonez, Joseph Redmon, and Ali Farhadi. Xnor-net: Imagenet classification using binary convolutional neural networks. In Bastian Leibe, Jiri Matas, Nicu Sebe, and Max Welling, editors, *Computer Vision – ECCV 2016*, pages 525–542, Cham, 2016. Springer International Publishing. ISBN 978-3-319-46493-0.
- [49] Mark Sandler, Andrew Howard, Menglong Zhu, Andrey Zhmoginov, and Liang Chieh Chen. MobileNetV2: Inverted Residuals and Linear Bottlenecks. *Proceedings of the IEEE Computer Society Conference on Computer Vision and Pattern Recognition*, pages 4510–4520, 2018. ISSN 10636919. doi: 10.1109/CVPR.2018.00474.

- [50] Jun Shi, Jianfeng Xu, Kazuyuki Tasaka, and Zhibo Chen. Sasl: Saliency-adaptive sparsity learning for neural network acceleration. *IEEE Transactions on Circuits and Systems for Video Technology*, 31(5):2008–2019, 2021. doi: 10.1109/TCSVT.2020.3013170.
- [51] Xavier Suau, Luca Zappella, and Nicholas Apostoloff. Network Compression using Correlation Analysis of Layer Responses. 2018.
- [52] Cheng Tai, Tong Xiao, Yi Zhang, Xiaogang Wang, et al. Convolutional neural networks with low-rank regularization. *arXiv preprint arXiv:1511.06067*, 2015.
- [53] Mingxing Tan and Quoc V Le. Efficientnet: Rethinking model scaling for convolutional neural networks. *arXiv preprint arXiv:1905.11946*, 2019.
- [54] Frederick Tung and Greg Mori. Clip-q: Deep network compression learning by in-parallel pruning-quantization. In *Proceedings of the IEEE Conference on Computer Vision and Pattern Recognition*, pages 7873–7882, 2018.
- [55] Jingdong Wang, Ke Sun, Tianheng Cheng, Borui Jiang, Chaorui Deng, Yang Zhao, Dong Liu, Yadong Mu, Mingkui Tan, Xinggang Wang, et al. Deep high-resolution representation learning for visual recognition. *IEEE transactions on pattern analysis and machine intelligence*, 2020.
- [56] Wei Wen, Cong Xu, Chunpeng Wu, Yandan Wang, Yiran Chen, and Hai Li. Coordinating filters for faster deep neural networks. In *The IEEE International Conference on Computer Vision (ICCV)*, Oct 2017.
- [57] Saining Xie, Ross Girshick, Piotr Dollár, Zhuowen Tu, and Kaiming He. Aggregated residual transformations for deep neural networks. *Proceedings - 30th IEEE Conference on Computer Vision and Pattern Recognition, CVPR 2017*, 2017-January:5987–5995, 2017. doi: 10.1109/CVPR.2017.634.
- [58] Zhonghui You, Kun Yan, Jinmian Ye, Meng Ma, and Ping Wang. Gate decorator: Global filter pruning method for accelerating deep convolutional neural networks, 2019.
- [59] Ruichi Yu, Ang Li, Chun-Fu Chen, Jui-Hsin Lai, Vlad I. Morariu, Xintong Han, Mingfei Gao, Ching-Yung Lin, and Larry S. Davis. Nisp: Pruning networks using neuron importance score propagation. In *The IEEE Conference on Computer Vision and Pattern Recognition (CVPR)*, June 2018.
- [60] Xiyu Yu, Tongliang Liu, Xinchao Wang, and Dacheng Tao. On compressing deep models by low rank and sparse decomposition. In *The IEEE Conference on Computer Vision and Pattern Recognition (CVPR)*, July 2017.
- [61] Tianyun Zhang, Shaokai Ye, Kaiqi Zhang, Jian Tang, Wujie Wen, Makan Fardad, and Yanzhi Wang. A systematic dnn weight pruning framework using alternating direction method of multipliers. In *Proceedings of the European Conference on Computer Vision (ECCV)*, pages 184–199, 2018.
- [62] Zhuangwei Zhuang, Mingkui Tan, Bohan Zhuang, Jing Liu, Yong Guo, Qingyao Wu, Junzhou Huang, and Jinhui Zhu. Discrimination-aware channel pruning for deep neural networks. In *Advances in Neural Information Processing Systems*, pages 875–886, 2018.

1 Proof of Lemma 1

Proof. For each input channel i , given an additive perturbation matrix $\Delta \mathbf{I}_i$, let $\tilde{\mathbf{I}}_i = \mathbf{I}_i + \Delta \mathbf{I}_i$. Given optimal parameters of kernel j expressed as $\mathbf{w}_j^{(i)} = \sum_{k=1}^r a_{k,j}^{(i)} \mathbf{u}_k^{(i)}$, which are learned from the training data, the output of the convolutional layer is

$$\begin{aligned} \mathbf{I}_j &= \sum_i (\mathbf{I}_i + \Delta \mathbf{I}_i) * \mathbf{w}_j^{(i)} = \sum_i (\mathbf{I}_i + \Delta \mathbf{I}_i) * \sum_{k=1}^r a_{k,j}^{(i)} \mathbf{u}_k^{(i)} \\ &= \sum_i \mathbf{I}_i * \sum_{k=1}^r a_{k,j}^{(i)} \mathbf{u}_k + \sum_i \Delta \mathbf{I}_i * \sum_{k=1}^r a_{k,j}^{(i)} \mathbf{u}_k^{(i)} \\ &= \mathbf{I}_j^* + \underbrace{\sum_i \Delta \mathbf{I}_i * \sum_{k=1}^r a_{k,j}^{(i)} \mathbf{u}_k^{(i)}}_{\text{perturbation term}} \end{aligned}$$

where \mathbf{I}_j^* denotes the optimal feature map. By using the infinity norm to characterize the effect of the perturbation, we have:

$$\|\mathbf{I}_j^* - \mathbf{I}_j\|_\infty = \left\| \sum_i \Delta \mathbf{I}_i * \sum_{k=1}^r a_{k,j}^{(i)} \mathbf{u}_k^{(i)} \right\|_\infty \quad (1)$$

$$\leq \sum_i \left\| \Delta \mathbf{I}_i * \sum_{k=1}^r a_{k,j}^{(i)} \mathbf{u}_k^{(i)} \right\|_\infty \quad (2)$$

From Young's inequality:

$$\begin{aligned} (1) &\leq \sum_i \|\Delta \mathbf{I}_i\|_2 \left\| \sum_{k=1}^r a_{k,j}^{(i)} \mathbf{u}_k^{(i)} \right\|_2 \\ &\leq \sum_i \|\Delta \mathbf{I}_i\|_2 \left\| \sum_{k=1}^r a_{k,j}^{(i)} \mathbf{u}_k^{(i)} \right\|_2 \\ &\leq \sum_i \|\Delta \mathbf{I}_i\|_2 \sum_{k=1}^r |a_{k,j}^{(i)}| \|\mathbf{u}_k^{(i)}\|_2 \\ &\leq \sum_i \|\Delta \mathbf{I}_i\|_2 \sum_{k=1}^r |a_{k,j}^{(i)}| \|\mathbf{u}_k^{(i)}\|_F \quad (3) \\ &\leq \sum_i \|\Delta \mathbf{I}_i\|_2 \|\mathbf{a}_j^{(i)}\|_1 \sum_{k=1}^r \|\mathbf{u}_k^{(i)}\|_F \end{aligned}$$

where $\mathbf{a}_j^{(i)} = [a_{1,j}^{(i)} \ \dots \ a_{r,j}^{(i)}]^\top$ and $\|\cdot\|_F$ denotes the Frobenius norm. Let $\bar{\mathbf{u}}_k^{(i)} = \text{vect}(\mathbf{u}_k^{(i)})$, where $\text{vect}(\cdot)$ denotes the vectorization of a matrix. If $\bar{\mathbf{U}}^{(i)\top} \bar{\mathbf{U}}^{(i)} = \mathbf{I}$, we have $\|\bar{\mathbf{u}}_k^{(i)}\|_F = 1$ and hence

$$(3) \leq \sum_i r \|\mathbf{a}_j^{(i)}\|_1 \|\Delta \mathbf{I}_i\|_2 \leq \sum_i r h \|\mathbf{a}_j^{(i)}\|_2 \|\Delta \mathbf{I}_i\|_2$$

where h is the kernel size. If $\|\mathbf{a}_j^{(i)}\|_2 \leq \epsilon, \forall i, j$, then

$$\left\| \sum_i \Delta \mathbf{I}_i * \mathbf{w}_j^{(i)} \right\|_\infty \leq \epsilon h r \sum_i \|\Delta \mathbf{I}_i\|_2$$

□

2 Network compression using DeCEF layers

One application of DeCEF is to use it as a model reduction technique for a pre-trained network. As discussed in the paper, this is not the main focus of DeCEF. Nevertheless, we propose an algorithm as follows for this type of applications.

Algorithm 1. (*DeCEFC-basenet*)

Step 1: *Analysis described in Procedure 1.*

Step 2: *For each layer, let $\bar{\mathbf{u}}_k^{(i)}$ be the columns of $\bar{\mathbf{U}}^{(i)}$. Approximate $\mathbf{w}_j^{(i)}$ by $\mathbf{w}_j^{(i)} \approx \sum_{k=1}^{r_i} a_{k,j}^{(i)} \mathbf{u}_k^{(i)}$, where $\mathbf{u}_k^{(i)}$ is obtained by reshaping $\bar{\mathbf{u}}_k^{(i)}$ into a $h \times h$ matrix.*

Step 3 (optional): *Network fine-tuning by freezing the eigen-filters and training the other trainable parameters.*

3 Demonstration of singular values computed using Procedure 1

Figure 1 shows the density histogram of singular values computed using Eq. [1] in the paper. The histogram is calculated from all input channels in each convolutional layer with $K > 1$. The maximum ranks of the layers in these example networks are $\min(K, c_{\text{out}}) = K$, where $K = 9$. Similar low rank behaviors can be observed in Fig. 2.

4 Convergence video

In this supplementary material, we include videos (in the file called “effective_rank_converge_video.zip”) to show some examples of how the effective ranks (cf. Eq.[2] in the paper) in each layer converge over training epochs. The title of each video indicates the layer index, i.e. the larger the index, the deeper the layer is. The network and data used here are the DenseNet-121 and ImageNet, respectively.

In the video, the leftmost rectangular box shows the singular values computed from all the output channels (filters) for each input channel. Each row in this figure contains the singular values for one input channel. The image in the middle is the histogram density of the effective rank. Each frame in this video shows the singular values and effective ranks computed from one epoch. Finally, the image on the right shows the convergence of this effective rank over raining epochs. Note that due to the limit on the file size, we only show the convergence for every fourth layer.



Figure 1: The density histogram (y-axis $\in [0, 1]$) of the effective rank (x-axis $\in [1, 9]$) estimated using Eq. [2] in Procedure 1 for DenseNet-121 trained on ImageNet. The statistics are computed over all input channels i in that layer. We see the decreasing trend of the effective ranks with respect to the depth of the network.

5 Summary of results

In this section, we present more detailed results from our experiments. Result comparisons can be found in Tab. 1 and Tab. 2 for CIFAR-10 and ImageNet, respectively. These results are also summarized as ball charts in Fig. 3 for CIFAR-10 and in Fig. 5 and Fig. 4 for ImageNet.

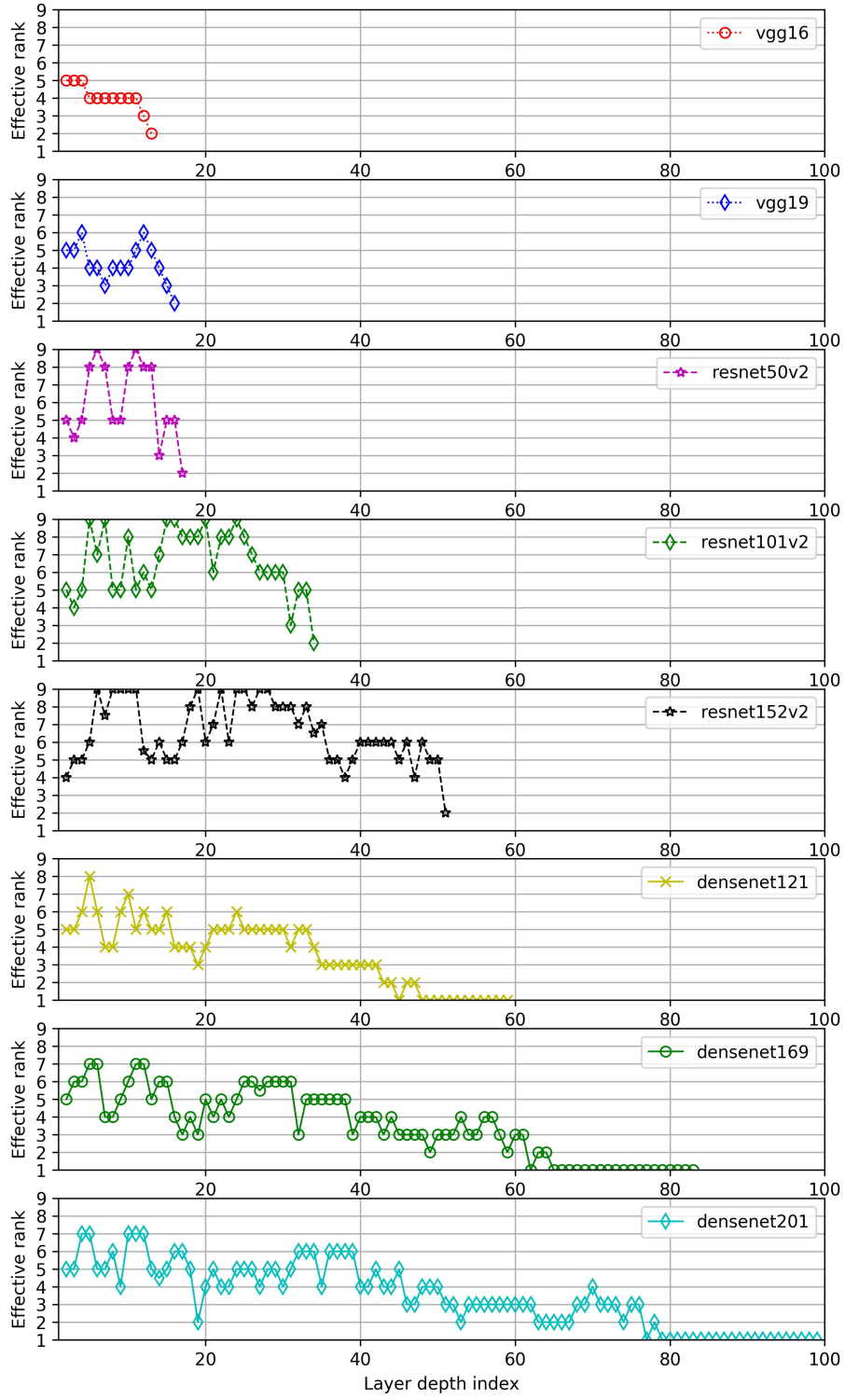


Figure 2: Effective rank (cf. Eq. [3] in the paper) versus layer depth. In these networks, we observe decreasing trend of the effective ranks when a network goes deeper. In this figure, we show this effect in the networks VGG, ResNet and DenseNet.

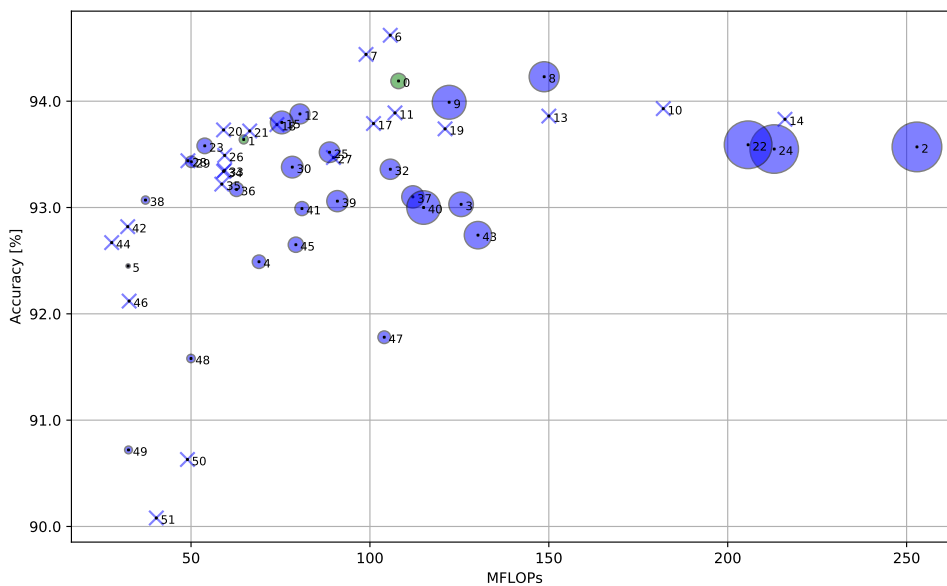


Figure 3: Accuracy (y-axis) versus FLOPs (x-axis) and number of trainable parameters (indicated by the radius of each ball) for CIFAR-10. Algorithms that have not reported their number of parameters are denoted as crosses (x) in the chart. More details can be found in Table 1. The number in the ball chart is the id of the algorithm that is indicated as the superscript in the table.

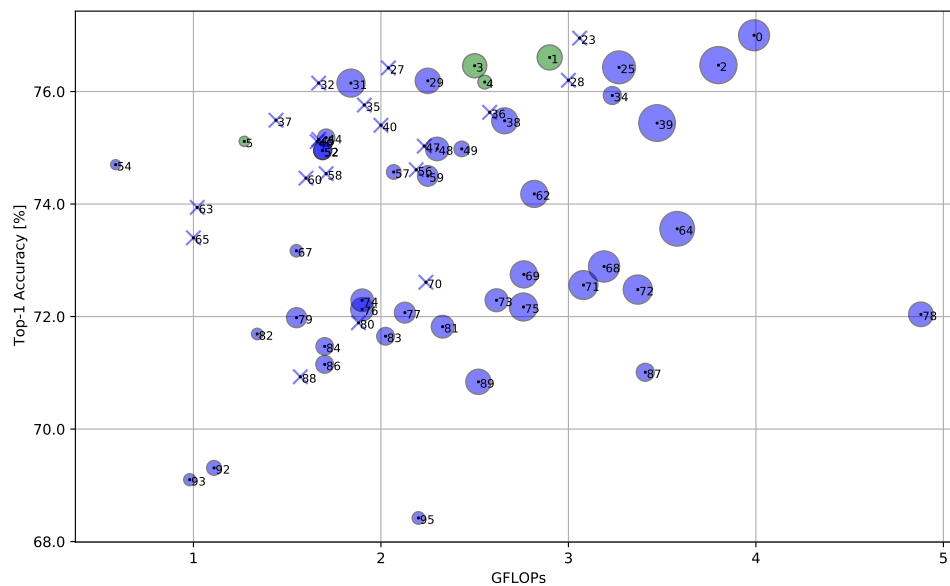


Figure 4: Top-1 accuracy (y-axis) versus FLOPs (x-axis) and number of trainable parameters (indicated by the radius of each ball) for ImageNet. Algorithms that have not reported their number of parameters are denoted as crosses (x) in the chart. More details can be found in Table 2. The number in the ball chart is the id of the algorithm that is indicated as the superscript in the table.

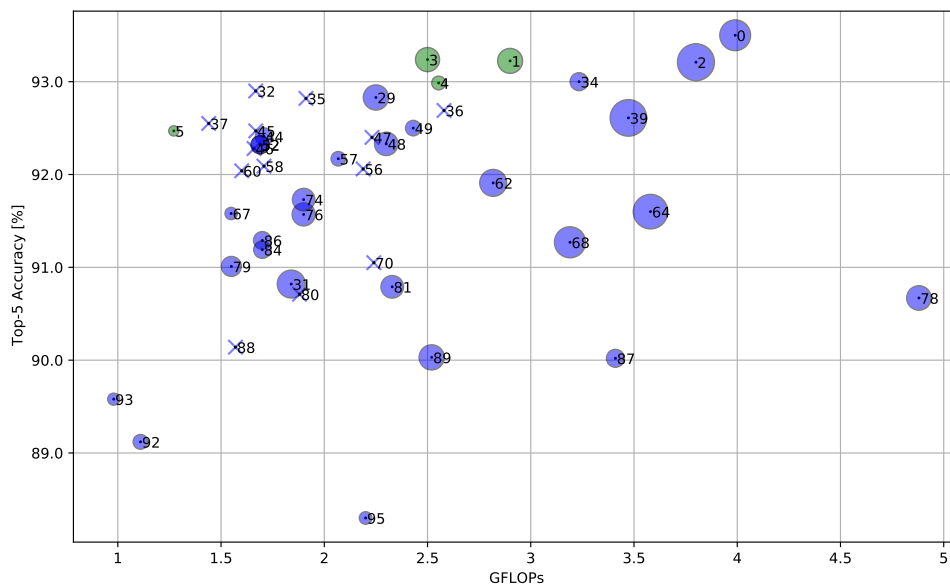


Figure 5: Top-5 accuracy (y-axis) versus FLOPs (x-axis) and number of trainable parameters (indicated by the radius of each ball) for ImageNet. Algorithms that have not reported their number of parameters are denoted as crosses (x) in the chart. More details can be found in Table 2. The number in the ball chart is the id of the algorithm that is indicated as the superscript in the table.

Table 1: Comparison to related work on CIFAR-10 dataset. Part (a): our networks refer to DeCEF with number of filters for each bock in the parenthesis ($c_{out,1}$, $c_{out,2}$, $c_{out,3}$), where $c_{out,b}$ is the number of filters in the layers from ResNet-32 block b . We train the baseline network ResNet-32 for comparison. Part (b): state-of-the-art results reported in literatures.

Network	Acc.	Std.	No. param.	MFLOPs
(a) DeCEF vs baseline network				
DeCEF-ResNet-32 (32, 64, 128) ⁰	94.19 %	(0.18 %)	533.00 k	108.00
DeCEF-ResNet-32 (24, 48, 96) ¹	93.64 %	(0.16 %)	311.00 k	64.72
ResNet-110 ² [8]	93.57 %		1.72 M	252.89
ResNet-56 ³ [8]	93.03 %		850.00 k	125.49
ResNet-32 ⁴ [8]	92.49 %		467.00 k	69.00
DeCEF-ResNet-32 (16, 32, 64) ⁵	92.45 %	(0.17 %)	148.00 k	32.42
(b) Related work				
ResRep ResNet-110 ⁶ [7]	94.62 %			105.68
C-SGD-5/8 ResNet-110 ⁷ [5]	94.44 %			98.91
HRank ResNet-110 1 ⁸ [18]	94.23 %		1.04 M	148.70
SASL ResNet-110 ⁹ [28]	93.99 %		1.17 M	122.15
SFP ResNet-110 20% ¹⁰ [10]	93.93 %			182.00
SFP ResNet-56 10% ¹¹ [10]	93.89 %			107.00
SASL ResNet-56 ¹² [28]	93.88 %		689.35 k	80.44
SFP ResNet-110 30% ¹³ [10]	93.86 %			150.00
SFP ResNet-110 10% ¹⁴ [10]	93.83 %			216.00
SASL* ResNet-110 ¹⁵ [28]	93.80 %		786.04 k	75.36
ShaResNet-164 ¹⁶ [2]	93.80 %		930.00 k	
LFPC ResNet-110 ¹⁷ [12]	93.79 %			101.00
SFP ResNet-56 30% ¹⁸ [10]	93.78 %			74.00
FPGM-only 40% ResNet-110 ¹⁹ [11]	93.74 %			121.00
ResRep ResNet-56 1 ²⁰ [7]	93.73 %			59.09
LFPC ResNet-56 1 ²¹ [12]	93.72 %			66.40
GAL-0.1 ResNet-110 ²² [21]	93.59 %		1.65 M	205.70
SASL* ResNet-56 ²³ [28]	93.58 %		538.90 k	53.84
ResNet-110-pruned-A ²⁴ [17]	93.55 %		1.68 M	213.00
HRank ResNet-56 1 ²⁵ [18]	93.52 %		710.00 k	88.72
FPGM-only 40% ResNet-56 ²⁶ [11]	93.49 %			59.40
SFP ResNet-56 20% ²⁷ [10]	93.47 %			89.80
C-SGD-5/8 ResNet-56 ²⁸ [5]	93.44 %			49.13
GBN-40 ²⁹ [32]	93.43 %		395.25 k	50.07
GAL-0.6 ResNet-56 ³⁰ [21]	93.38 %		750.00 k	78.30
NISP-110 ³¹ [33]	93.38 %		976.10 k	
HRank ResNet-110 2 ³² [18]	93.36 %		700.00 k	105.70
SFP ResNet-56 40% ³³ [10]	93.35 %			59.40
LFPC ResNet-56 2 ³⁴ [12]	93.34 %			59.10
SFP ResNet-32 10% ³⁵ [10]	93.22 %			58.60
HRank ResNet-56 2 ³⁶ [18]	93.17 %		490.00 k	62.72
ResNet-56-pruned-A ³⁷ [17]	93.10 %		770.10 k	112.00
GBN-30 ³⁸ [32]	93.07 %		283.05 k	37.27
ResNet-56-pruned-B ³⁹ [17]	93.06 %		733.55 k	90.90
ResNet-110-pruned-B ⁴⁰ [17]	93.00 %		1.16 M	115.00
NISP-56 ⁴¹ [33]	92.99 %		487.90 k	81.00
FPGM-mix 40% ResNet-32 ⁴² [11]	92.82 %			32.30
GAL-0.5 ResNet-110 ⁴³ [21]	92.74 %		950.00 k	130.20
ResRep ResNet-56 2 ⁴⁴ [7]	92.67 %			27.82
HRank ResNet-110 3 ⁴⁵ [18]	92.65 %		530.00 k	79.30
LFPC ResNet-32 ⁴⁶ [12]	92.12 %			32.70
nin-c3-lr ⁴⁷ [16]	91.78 %		438.00 k	104.00
GAL-0.8 ResNet-56 ⁴⁸ [21]	91.58 %		290.00 k	49.99
HRank ResNet-56 3 ⁴⁹ [18]	90.72 %		270.00 k	32.52
SFP ResNet-32 20% ⁵⁰ [10]	90.63 %			49.00
SFP ResNet-32 30% ⁵¹ [10]	90.08 %			40.30

Table 2: Comparison to state-of-the-art techniques on the dataset ImageNet (ILSVRC-2012). “DeCEF (linear decay)” and “DeCEF (log decay)” refer to training a network using Algorithm 1 with linear and log decay, respectively, and “DeCEFC” refers to the network compression using Algorithm 1. *Official Tensorflow[1] implementation.

Network	Top-5 Acc.	Std.	Top-1 Acc.	Std.	No. param.	GFLOPs
(a) DeCEF vs baseline network						
HRNet-W18-C ⁹ [31]	93.50%		77.00%		21.30 M	3.99
DeCEF-ResNet-50 (lin decay) ¹	93.22%	(0.07%)	76.61%	(0.06%)	17.27 M	2.90
ResNet-50 ² [9]	93.21%		76.47%		25.56 M	3.80
DeCEF-ResNet-50 (log decay) ³	93.24%	(0.05%)	76.46%	(0.05%)	16.64 M	2.50
DeCEF-HRNet-W18-C (lin decay) ⁴	92.99%		76.17%		9.49 M	2.55
DeCEF-HRNet-W18-C (log decay) ⁵	92.47%		75.11%		7.05 M	1.27
(b) Related work						
EfficientNet-B7 ⁶ [30]	96.84%		84.43%		64.10 M	
EfficientNet-B6 ⁷ [30]	96.90%		84.08%		41.00 M	
EfficientNet-B5 ⁸ [30]	96.71%		83.70%		28.50 M	
EfficientNet-B4 ⁹ [30]	96.26%		82.96%		17.70 M	
NASNet-Large ¹⁰ [37]	96.00%		82.50%		84.90 M	
EfficientNet-B3 ¹¹ [30]	95.68%		81.58%		10.80 M	
InceptionResNetV2 ¹² [4]	95.25%		80.26%		54.30 M	
EfficientNet-B2 ¹³ [30]	94.95%		80.18%		7.80 M	
EfficientNet-B1 ¹⁴ [30]	94.45%		79.13%		6.60 M	
Xception ¹⁵ [3]	94.50%		79.00%		22.86 M	
ResNet152V2 ¹⁶ [9]	94.16%		78.03%		58.30 M	
InceptionV3 ¹⁷ [29]	93.72%		77.90%		21.80 M	
ShuffleNet-152 ¹⁸ [2]	93.86%		77.77%		36.80 M	
DenseNet201 ¹⁹ [14]	93.62%		77.32%		18.30 M	
ResNet101V2 ²⁰ [9]	93.82%		77.23%		42.60 M	
EfficientNet-B0 ²¹ [30]	93.49%		77.19%		4.00 M	
ShuffleNet-101 ²² [2]	93.45%		77.09%		29.40 M	
GFP ResNet-50 1 ²³ [22]			76.95%			3.06
ResNet152 ²⁴ [8]	93.12%		76.60%		58.40 M	
Taylor-FO-BN-91 ²⁵ [26]			76.43%		22.60 M	3.27
ResNet101 ²⁶ [8]	92.79%		76.42%		42.70 M	
GFP ResNet-50 2 ²⁷ [22]			76.42%			2.04
MetaPruning 0.85 ResNet-50 ²⁸ [23]			76.20%			3.00
GBN-60 ²⁹ [32]	92.83%		76.19%		17.42 M	2.25
DenseNet169 ³⁰ [14]	93.18%		76.18%		12.60 M	
ResNet-50 GAL-0.5-joint ³¹ [21]	90.82%		76.15%		19.31 M	1.84
ResRep ResNet-50 1 ³² [7]	92.90%		76.15%			1.67
ResNet50V2 ³³ [9]	93.03%		75.96%		23.60 M	
SSS-ResNetXi-41 ³⁴ [15]	93.00%		75.93%		12.40 M	3.23
SASL ³⁵ [28]	92.82%		75.76%			1.91
AOFP-C1 ³⁶ [6]	92.69%		75.63%			2.58
ResRep ResNet-50 2 ³⁷ [7]	92.55%		75.49%			1.44
Taylor-FO-BN-81 ³⁸ [26]			75.48%		17.90 M	2.66
SSS-ResNet-41 ³⁹ [15]	92.61%		75.44%		25.30 M	3.47
MetaPruning 0.75 ResNet-50 ⁴⁰ [23]			75.40%			2.00
ShuffleNet-50 ⁴¹ [2]	92.59%		75.39%		20.50 M	
MobileNetV2(alpha=1.4) ⁴² [27]	92.42%		75.23%		4.40 M	
ResNet-50 Variational ⁴³ [35]	92.10%		75.20%		15.30 M	
GBN-50 ⁴⁴ [32]	92.41%		75.18%		11.91 M	1.71
SASL ⁴⁵ [28]	92.47%		75.15%			1.67
AOFP-C2 ⁴⁶ [6]	92.28%		75.11%			1.66
ResNet-50 FPGM-only 30% ⁴⁷ [111]	92.40%		75.03%			2.23
ResNet-50 HRank 1 ⁴⁸ [18]	92.33%		74.98%		16.15 M	2.30
SSS-ResNetXi-38 ⁴⁹ [15]	92.50%		74.98%		10.70 M	2.43
DenseNet121 ⁵⁰ [14]	92.26%		74.97%		7.00 M	
DCP ⁵¹ [36]	92.32%		74.95%		12.41 M	1.69
DCP ⁵² [36]	92.32%		74.93%		12.41 M	1.69
ResNet50 ⁵³ [8]	92.06%		74.93%		23.60 M	
MobileNetV2 ⁵⁴ [27]			74.70%		6.90 M	0.58
MobileNetV2(alpha=1.3) ⁵⁵ [27]	92.12%		74.68%		3.80 M	
SFP ⁵⁶ [10]	92.06%		74.61%			2.19
SSS-ResNetXi-35-A ⁵⁷ [15]	92.17%		74.57%		10.00 M	2.07
C-SGD-50 ⁵⁸ [5]	92.09%		74.54%			1.71
Taylor-FO-BN-72 ⁵⁹ [26]			74.50%		14.20 M	2.25
LFPC ⁶⁰ [12]	92.04%		74.46%			1.60
NASNetMobile ⁶¹ [37]	91.85%		74.37%		4.30 M	
SSS-ResNet-32 ⁶² [15]	91.91%		74.18%		18.60 M	2.82
GFP ResNet-50 3 ⁶³ [22]			73.94%			1.02
Pruned-90 ⁶⁴ [24]	91.60%		73.56%		23.89 M	3.58
MetaPruning 0.5 ResNet-50 ⁶⁵ [23]			73.40%			1.00
ShuffleNet-34 ⁶⁶ [2]	90.58%		73.27%		13.60 M	
SSS-ResNetXi-35-B ⁶⁷ [15]	91.58%		73.17%		8.50 M	1.55
Pruned-75 ⁶⁸ [24]	91.27%		72.89%		21.47 M	3.19
NISP-50-A ⁶⁹ [33]			72.75%		18.63 M	2.76
GDP 0.7 ⁷⁰ [19]	91.05%		72.61%			2.24
ResNet-34-pruned-A ⁷¹ [17]			72.56%		19.90 M	3.08
ResNet-34-pruned-C ⁷² [17]			72.48%		20.10 M	3.37
NISP-34-A ⁷³ [33]			72.29%		15.74 M	2.62
ResNet-50 SSR-L2.0 A ⁷⁴ [20]	91.73%		72.29%		15.50 M	1.90
ResNet-34-pruned-B ⁷⁵ [17]			72.17%		19.30 M	2.76
ResNet-50 SSR-L2.1 A ⁷⁶ [20]	91.57%		72.13%		15.90 M	1.90
NISP-50-B ⁷⁷ [33]			72.07%		14.36 M	2.13
ThiNet-70 ⁷⁸ [25]	90.67%		72.04%		16.94 M	4.88
ResNet-50 HRank 2 ⁷⁹ [18]	91.01%		71.98%		13.77 M	1.55
GDP 0.6 ⁸⁰ [19]	90.71%		71.89%			1.88
SSS-ResNet-26 ⁸¹ [15]	90.79%		71.82%		15.60 M	2.33
Taylor-FO-BN-56 ⁸² [26]			71.69%		7.90 M	1.34
NISP-34-B ⁸³ [33]			71.65%		12.17 M	2.02
ResNet-50 SSR-L2.0 B ⁸⁴ [20]	91.19%		71.47%		12.00 M	1.70
MobileNetV2(alpha=1.0) ⁸⁵ [27]	90.14%		71.34%		2.30 M	
ResNet-50 SSR-L2.1 B ⁸⁶ [20]	91.29%		71.15%		12.20 M	1.70
ThiNet-50 ⁸⁷ [25]	90.02%		71.01%		12.38 M	3.41
GDP 0.5 ⁸⁸ [19]	90.14%		70.93%			1.57
Pruned-50 ⁸⁹ [24]	90.03%		70.84%		17.38 M	2.52
MobileNet(alpha=1.0) ⁹⁰ [13]	89.50%		70.42%		3.20 M	
MobileNetV2(alpha=0.75) ⁹¹ [27]	89.18%		69.53%		1.40 M	
ResNet-50 GAL-1-joint ⁹² [21]	89.12%		69.31%		10.21 M	1.11
ResNet-50 HRank 3 ⁹³ [18]	89.58%		69.10%		8.27 M	0.98
GreBdec (VGG-16) ⁹⁴ [34]	89.06%		68.75%		9.70 M	
ThiNet-30 ⁹⁵ [25]	88.30%		68.42%		8.66 M	2.20
MobileNet(alpha=0.75) ⁹⁶ [13]	88.24%		68.41%		1.80 M	
GreBdec (GoogLeNet) ⁹⁷ [34]	88.11%		68.30%		1.50 M	

References

- [1] Martín Abadi, Ashish Agarwal, Paul Barham, Eugene Brevdo, Zhifeng Chen, Craig Citro, Greg S. Corrado, Andy Davis, Jeffrey Dean, Matthieu Devin, Sanjay Ghemawat, Ian Goodfellow, Andrew Harp, Geoffrey Irving, Michael Isard, Yangqing Jia, Rafal Jozefowicz, Lukasz Kaiser, Manjunath Kudlur, Josh Levenberg, Dandelion Mané, Rajat Monga, Sherry Moore, Derek Murray, Chris Olah, Mike Schuster, Jonathon Shlens, Benoit Steiner, Ilya Sutskever, Kunal Talwar, Paul Tucker, Vincent Vanhoucke, Vijay Vasudevan, Fernanda Viégas, Oriol Vinyals, Pete Warden, Martin Wattenberg, Martin Wicke, Yuan Yu, and Xiaoqiang Zheng. TensorFlow: Large-scale machine learning on heterogeneous systems, 2015. Software available from tensorflow.org.
- [2] Alexandre Boulch. Reducing parameter number in residual networks by sharing weights. *Pattern Recognition Letters*, 103:53 – 59, 2018. ISSN 0167-8655. doi: <https://doi.org/10.1016/j.patrec.2018.01.006>.
- [3] Francois Chollet. Xception: Deep learning with depthwise separable convolutions. In *The IEEE Conference on Computer Vision and Pattern Recognition (CVPR)*, July 2017.
- [4] Szegedy Christian, Ioffe Sergey, Vanhoucke Vincent, and Alemi Alexander. Inception-v4, inception-resnet and the impact of residual connections on learning, 2017.
- [5] Xiaohan Ding, Guiguang Ding, Yuchen Guo, and Jungong Han. Centripetal sgd for pruning very deep convolutional networks with complicated structure. In *Proceedings of the IEEE Conference on Computer Vision and Pattern Recognition*, pages 4943–4953, 2019.
- [6] Xiaohan Ding, Guiguang Ding, Yuchen Guo, Jungong Han, and Chenggang Yan. Approximated oracle filter pruning for destructive CNN width optimization. In Kamalika Chaudhuri and Ruslan Salakhutdinov, editors, *Proceedings of the 36th International Conference on Machine Learning*, volume 97 of *Proceedings of Machine Learning Research*, pages 1607–1616. PMLR, 09–15 Jun 2019.
- [7] Xiaohan Ding, Tianxiang Hao, Ji Liu, Jungong Han, Yuchen Guo, and Guiguang Ding. Lossless cnn channel pruning via gradient resetting and convolutional re-parameterization. *arXiv preprint arXiv:2007.03260*, 1, 2020.
- [8] K. He, X. Zhang, S. Ren, and J. Sun. Deep residual learning for image recognition. In *2016 IEEE Conference on Computer Vision and Pattern Recognition (CVPR)*, pages 770–778, June 2016. doi: 10.1109/CVPR.2016.90.
- [9] Kaiming He, Xiangyu Zhang, Shaoqing Ren, and Jian Sun. Identity mappings in deep residual networks. In *European conference on computer vision*, pages 630–645. Springer, 2016.
- [10] Yang He, Guoliang Kang, Xuanyi Dong, Yanwei Fu, and Yi Yang. Soft filter pruning for accelerating deep convolutional neural networks. *arXiv preprint arXiv:1808.06866*, 2018.
- [11] Yang He, Ping Liu, Ziwei Wang, Zhilan Hu, and Yi Yang. Filter pruning via geometric median for deep convolutional neural networks acceleration. In *Proceedings of the IEEE Conference on Computer Vision and Pattern Recognition*, pages 4340–4349, 2019.
- [12] Yang He, Yuhang Ding, Ping Liu, Linchao Zhu, Hanwang Zhang, and Yi Yang. Learning filter pruning criteria for deep convolutional neural networks acceleration. In *Proceedings of the IEEE/CVF Conference on Computer Vision and Pattern Recognition (CVPR)*, June 2020.

- [13] Andrew G Howard, Menglong Zhu, Bo Chen, Dmitry Kalenichenko, Weijun Wang, Tobias Weyand, Marco Andreetto, and Hartwig Adam. Mobilenets: Efficient convolutional neural networks for mobile vision applications. *arXiv preprint arXiv:1704.04861*, 2017.
- [14] Gao Huang, Zhuang Liu, Laurens van der Maaten, and Kilian Q. Weinberger. Densely connected convolutional networks, 2016.
- [15] Zehao Huang and Naiyan Wang. Data-driven sparse structure selection for deep neural networks. In *Proceedings of the European conference on computer vision (ECCV)*, pages 304–320, 2018.
- [16] Yani Ioannou, Duncan Robertson, Jamie Shotton, Roberto Cipolla, and Antonio Criminisi. Training cnns with low-rank filters for efficient image classification. *arXiv preprint arXiv:1511.06744*, 2015.
- [17] Hao Li, Asim Kadav, Igor Durdanovic, Hanan Samet, and Hans Peter Graf. Pruning filters for efficient convnets. *arXiv preprint arXiv:1608.08710*, 2016.
- [18] Mingbao Lin, Rongrong Ji, Yan Wang, Yichen Zhang, Baochang Zhang, Yonghong Tian, and Ling Shao. Hrank: Filter pruning using high-rank feature map. In *Proceedings of the IEEE/CVF Conference on Computer Vision and Pattern Recognition*, pages 1529–1538, 2020.
- [19] Shaohui Lin, Rongrong Ji, Yuchao Li, Yongjian Wu, Feiyue Huang, and Baochang Zhang. Accelerating convolutional networks via global & dynamic filter pruning. In *IJCAI*, pages 2425–2432, 2018.
- [20] Shaohui Lin, Rongrong Ji, Yuchao Li, Cheng Deng, and Xuelong Li. Toward compact convnets via structure-sparsity regularized filter pruning. *IEEE transactions on neural networks and learning systems*, 31(2):574–588, 2019.
- [21] Shaohui Lin, Rongrong Ji, Chenqian Yan, Baochang Zhang, Liujuan Cao, Qixiang Ye, Feiyue Huang, and David Doermann. Towards optimal structured cnn pruning via generative adversarial learning. In *Proceedings of the IEEE Conference on Computer Vision and Pattern Recognition*, pages 2790–2799, 2019.
- [22] Liyang Liu, Shilong Zhang, Zhanghui Kuang, Aojun Zhou, Jing-Hao Xue, Xinjiang Wang, Yimin Chen, Wenming Yang, Qingmin Liao, and Wayne Zhang. Group fisher pruning for practical network compression. In Marina Meila and Tong Zhang, editors, *Proceedings of the 38th International Conference on Machine Learning*, volume 139 of *Proceedings of Machine Learning Research*, pages 7021–7032. PMLR, 18–24 Jul 2021.
- [23] Zechun Liu, Haoyuan Mu, Xiangyu Zhang, Zichao Guo, Xin Yang, Kwang-Ting Cheng, and Jian Sun. Metapruning: Meta learning for automatic neural network channel pruning. In *Proceedings of the IEEE International Conference on Computer Vision*, pages 3296–3305, 2019.
- [24] Jian-Hao Luo and Jianxin Wu. An entropy-based pruning method for cnn compression. *arXiv preprint arXiv:1706.05791*, 2017.
- [25] Jian-Hao Luo, Jianxin Wu, and Weiyao Lin. Thinet: A filter level pruning method for deep neural network compression. In *Proceedings of the IEEE international conference on computer vision*, pages 5058–5066, 2017.
- [26] Pavlo Molchanov, Arun Mallya, Stephen Tyree, Iuri Frosio, and Jan Kautz. Importance estimation for neural network pruning. In *Proceedings of the IEEE/CVF Conference on Computer Vision and Pattern Recognition (CVPR)*, June 2019.

- [27] Mark Sandler, Andrew Howard, Menglong Zhu, Andrey Zhmoginov, and Liang Chieh Chen. MobileNetV2: Inverted Residuals and Linear Bottlenecks. *Proceedings of the IEEE Computer Society Conference on Computer Vision and Pattern Recognition*, pages 4510–4520, 2018. ISSN 10636919. doi: 10.1109/CVPR.2018.00474.
- [28] Jun Shi, Jianfeng Xu, Kazuyuki Tasaka, and Zhibo Chen. Sasl: Saliency-adaptive sparsity learning for neural network acceleration. *IEEE Transactions on Circuits and Systems for Video Technology*, 31(5): 2008–2019, 2021. doi: 10.1109/TCSVT.2020.3013170.
- [29] Christian Szegedy, Vincent Vanhoucke, Sergey Ioffe, Jon Shlens, and Zbigniew Wojna. Rethinking the inception architecture for computer vision. In *Proceedings of the IEEE conference on computer vision and pattern recognition*, pages 2818–2826, 2016.
- [30] Mingxing Tan and Quoc V Le. Efficientnet: Rethinking model scaling for convolutional neural networks. *arXiv preprint arXiv:1905.11946*, 2019.
- [31] Jingdong Wang, Ke Sun, Tianheng Cheng, Borui Jiang, Chaorui Deng, Yang Zhao, Dong Liu, Yadong Mu, Mingkui Tan, Xinggang Wang, et al. Deep high-resolution representation learning for visual recognition. *IEEE transactions on pattern analysis and machine intelligence*, 2020.
- [32] Zhonghui You, Kun Yan, Jinmian Ye, Meng Ma, and Ping Wang. Gate decorator: Global filter pruning method for accelerating deep convolutional neural networks, 2019.
- [33] Ruichi Yu, Ang Li, Chun-Fu Chen, Jui-Hsin Lai, Vlad I. Morariu, Xintong Han, Mingfei Gao, Ching-Yung Lin, and Larry S. Davis. Nisp: Pruning networks using neuron importance score propagation. In *The IEEE Conference on Computer Vision and Pattern Recognition (CVPR)*, June 2018.
- [34] Xiyu Yu, Tongliang Liu, Xinchao Wang, and Dacheng Tao. On compressing deep models by low rank and sparse decomposition. In *The IEEE Conference on Computer Vision and Pattern Recognition (CVPR)*, July 2017.
- [35] Chenglong Zhao, Bingbing Ni, Jian Zhang, Qiwei Zhao, Wenjun Zhang, and Qi Tian. Variational convolutional neural network pruning. In *Proceedings of the IEEE Conference on Computer Vision and Pattern Recognition*, pages 2780–2789, 2019.
- [36] Zhuangwei Zhuang, Mingkui Tan, Bohan Zhuang, Jing Liu, Yong Guo, Qingyao Wu, Junzhou Huang, and Jinhui Zhu. Discrimination-aware channel pruning for deep neural networks. In *Advances in Neural Information Processing Systems*, pages 875–886, 2018.
- [37] Barret Zoph, Vijay Vasudevan, Jonathon Shlens, and Quoc V Le. Learning transferable architectures for scalable image recognition. In *Proceedings of the IEEE conference on computer vision and pattern recognition*, pages 8697–8710, 2018.